INTERNATIONAL ATOMIC ENERGY AGENCY
UNITED NATIONS EDUCATIONAL, SCIENTIFIC AND CULTURAL ORGANIZATION
INTERNATIONAL CENTRE FOR THEORETICAL PHYSICS
I.C.T.P., P.O. BOX 586, 34100 TRIESTE, ITALY, CABLE: CENTRATOM TRIESTE

H4.SMR/841-2

FOURTH ICTP-URSI-ITU(BDT) COLLEGE ON RADIOPROPAGATION:
Propagation, Informatics and Radiocommunication System Planning

30 January - 3 March 1995

Miramare - Trieste, Italy

Fundamentals of Computer Techniques in Electromagnetics

F. Gardiol
Ecole Polytechnique Federal de Lausanne
Switzerland

FOURTH ICTP-URSI COLLEGE ON RADIOPROPAGATION

INTERNATIONAL CENTER FOR THEORETICAL PHYSICS

30 JANUARY- 3 MARCH 1955, TRIESTE, ITALY

FUNDAMENTALS OF COMPUTER TECHNIQUES IN ELECTROMAGNETICS

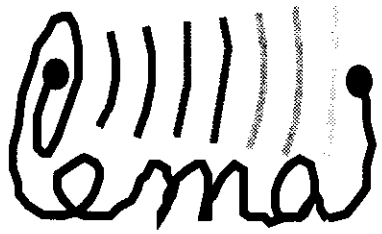

1: Transmission Lines, Input Impedance, Reflectionless Matching

2: Approximate Techniques for Electromagnetics - FDTD, TLM, MMP

3: Variational Principles - Finite Elements

4: Antennas and Arrays

5: Integral Equation Techniques - Mininec

6: Atmospheric Propagation

F. Gardiol, Professor,
Laboratoire d'Électromagnétisme et d'Acoustique (LEMA)
École Polytechnique Fédérale
ELB-Ecublens, CH-1015 Lausanne, Switzerland

LESSON 1, WEDNESDAY 1 FEBRUARY 1995

TRANSMISSION LINES, INPUT IMPEDANCE, MATCHING

Introduction

A transmission line is made of two or more conducting strips or wires, along which electrical signals travel with a velocity that is very large but finite. The transmission takes a certain amount of time, which becomes significant for high-frequency signals or fast pulses, and this delay affects the performance of the system.

Theoretical developments most often consider a lossless line, made with perfect electric conductors (PEC) and ideal insulating materials (perfect dielectrics). An ideal transmission line is formed by two metallic conductors, assumed to be straight and infinitely long, which are embedded in a homogeneous lossless dielectric. The conductor cross sections and the material parameters do not vary along the line (uniformity), so the transverse and the longitudinal dependences of the fields can be separated [1]. The longitudinal behavior defines the propagation of signals in terms of the transverse voltage and the current.

The frequency range over which a transmission line can be used is limited when higher order modes excited at discontinuities start to propagate or to radiate. The simultaneous propagation of several modes, with different velocities, produces a distortion of the signal, while radiation reduces the amplitude of a signal propagating along the line and can be the cause of spurious coupling.

The concepts derived when considering ideal lines remain approximately valid, with minor changes, for practical lines actually encountered in applications. Bending the lines does not cause major effects as long as the radii of the bends remain sufficiently large and the line cross section is not significantly altered.

Real materials are always slightly lossy and part of valuable signals is always transformed into useless heat. The main loss contribution is produced by Joule heating in the conductors, which all have some resistivity. No conduction current can flow across vacuum, and this is approximately also true for air. On the other hand, some current can flow across insulating material; it is most often negligible but increases when the material is damaged or wet.

Taking resistive and dielectric losses into account, an extremely short section of transmission line can be represented by the equivalent circuit of the figure 1.1.

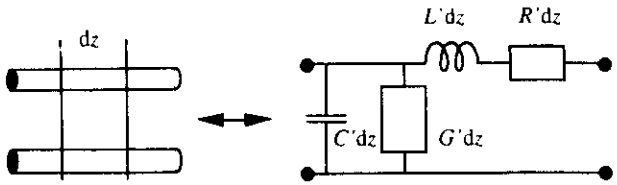

Fig. 1.1 Equivalent circuit of a lossy transmission line of length dz.

The application of Kirchhoff's lemmas to the equivalent circuit provides the two transmission line equations, which involve partial derivatives of the voltage and the current with respect to both the time and the position along the line. It is not possible to obtain a time-domain solution for the general case of the lossy line.

Alternating Currents in Complex Notation

The transmission line equations include both space and time derivatives. Their resolution becomes much simpler when the time derivative is removed. A voltage u, having a sinusoidal time dependence of angular frequency $\omega = 2\pi f$, is expressed by

$$u(z,t) = \sqrt{2}\, U_0(z)\cos(\omega t + \phi_u) \tag{1.1}$$

where U_0 is the effective amplitude and ϕ_u is the phase. The sine-wave time dependence can be expressed in complex notation, with Equation (4.10) written as:

$$u(z,t) = \mathrm{Re}\left[\sqrt{2}\,\underline{U}(z)\exp(\mathrm{j}\omega t)\right] \quad \text{with} \quad \underline{U}(z) = U_0(z)\exp\left[\mathrm{j}\phi_u(z)\right] \tag{1.2}$$

The current i is similarly expressed in complex notation:

$$i(z,t) = \mathrm{Re}\left[\sqrt{2}\,\underline{I}(z)\exp(\mathrm{j}\omega t)\right] \quad \text{with} \quad \underline{I}(z) = I_0(z)\exp\left[\mathrm{j}\phi_i(z)\right] \tag{1.3}$$

To distinguish complex variables (frequency domain) from real quantities and thus avoid confusions all *complex* quantities are underlined (IEC regulations)

Voltages and currents become complex functions called *phasors*. Their real part provides the value at time $t = 0$, and the imaginary part at $t = -T/4$ where $T = 1/f$ is the period. The derivation with respect to time yields a multiplying factor $\mathrm{j}\omega$: all time derivatives $\partial/\partial t$ of time-domain equations are replaced by $\mathrm{j}\omega$ in complex notation, also called *frequency-domain* notation (it would be completely incorrect, of course, to introduce complex quantities in time domain expressions or to encounter time derivatives in frequency domain formulations).

Equivalent circuit and transmission line equations in complex notation

The equivalent circuit of the transmission line (Fig. 1.1) can be put in a more general form (Fig. 1.2), with a linear series impedance $\underline{Z}' = R' + \mathrm{j}\omega L'$ and a linear shunt admittance $\underline{Y}' = G' + \mathrm{j}\omega C'$. The equivalent circuit $\underline{Y}'\underline{Z}'$ is more general and can also be used to simulate other propagation phenomena — for instance, a wave traveling in an homogeneous lossy medium or still propagation in metallic or dielectric waveguides.

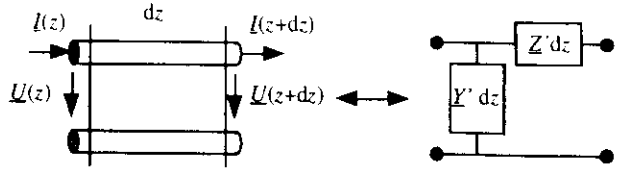

Figure 1.2 Equivalent circuit of a lossy transmission line of length dz.

The two transmission line equations then become, in complex notation, two total differential equations of first order:

$$\frac{\mathrm{d}\underline{I}(z)}{\mathrm{d}z} = -\underline{Y}'\,\underline{U}(z) = -(G' + \mathrm{j}\omega C')\underline{U}(z) \quad \text{and} \quad \frac{\mathrm{d}\underline{U}(z)}{\mathrm{d}z} = -\underline{Z}'\,\underline{I}(z) = -(R' + \mathrm{j}\omega L')\underline{I}(z) \tag{1.4}$$

The combination of the two equations (4.13) yields second-order differential wave equations either for the voltage or for the current:

$$\frac{\mathrm{d}^2\underline{U}(z)}{\mathrm{d}z^2} = \underline{Z}'\underline{Y}'\underline{U}(z) \qquad \frac{\mathrm{d}^2\underline{I}(z)}{\mathrm{d}z^2} = \underline{Z}'\underline{Y}'\underline{I}(z) \tag{1.5}$$

Solving (1.5) yields the voltage and the current phasors on a lossy transmission line.

$$\underline{U}(z) = \underline{U}_+ \mathrm{e}^{-\underline{\gamma}z} + \underline{U}_- \mathrm{e}^{+\underline{\gamma}z} \qquad \underline{I}(z) = \frac{1}{\underline{Z}_c}\left(\underline{U}_+ \mathrm{e}^{-\underline{\gamma}z} + \underline{U}_- \mathrm{e}^{+\underline{\gamma}z}\right) \tag{1.6}$$

where the propagation factor $\underline{\gamma}$ and the characteristic impedance $\underline{Z}_c$ are:

$$\underline{\gamma} = \sqrt{\underline{Z}'\underline{Y}'} = \alpha + \mathrm{j}\beta \qquad \underline{Z}_c = \frac{\underline{Z}'}{\underline{\gamma}} = \pm\sqrt{\frac{\underline{Z}'}{\underline{Y}'}} \tag{1.7}$$

For an LC line with R and G components related to losses, the attenuation factor α and the phase-shift factor β are given by

$$\alpha = \sqrt{\frac{1}{2}\sqrt{\left(R'^2+\omega^2L'^2\right)\left(G'^2+\omega^2C'^2\right)}+R'G'-\omega^2L'C'} \quad [\mathrm{m^{-1}}]$$

$$\beta = \sqrt{\frac{1}{2}\sqrt{\left(R'^2+\omega^2L'^2\right)\left(G'^2+\omega^2C'^2\right)}-R'G'+\omega^2L'C'} \quad [\mathrm{m^{-1}}] \qquad (1.8)$$

The first term in eqn. (1.6) corresponds to the forward wave, that travels towards increasing values of z while the second term corresponds to the backward wave that travels in the opposite direction.

The ratio of backward to forward waves is the reflection factor $\underline{\rho}(z)$:

$$\underline{\rho}(z) = \frac{\underline{U}_- e^{+\underline{\gamma}z}}{\underline{U}_+ e^{-\underline{\gamma}z}} = \frac{\underline{U}_-}{\underline{U}_+} e^{+2\underline{\gamma}z} = \underline{\rho}(0) e^{+2\underline{\gamma}z} \quad [1] \qquad (1.9)$$

the local impedance $\underline{Z}(z)$ is defined as the ratio of voltage to current at a point z on the line:

$$\underline{Z}(z) = \frac{\underline{U}(z)}{\underline{I}(z)} = \frac{\underline{U}_+ e^{-\underline{\gamma}z}\left[1+\underline{\rho}(z)\right]}{\underline{Y}_c \underline{U}_+ e^{-\underline{\gamma}z}\left[1-\underline{\rho}(z)\right]} = \underline{Z}_c \frac{1+\underline{\rho}(z)}{1-\underline{\rho}(z)} \quad [\Omega] \qquad (1.10)$$

Line of finite length

The length of a real transmission line is always finite. The boundary conditions at its two ends specify the two unknowns $\underline{U}_+$ and $\underline{U}_-$ and thus determine completely the voltage, the current and power distribution at every point along the line. At one end of the line, set generally at $z = 0$, the *generator*, or *source* generates the signal transmitted on the line. At the other end of the line at $x = d$ a *receiver* or *termination* absorbs the signal, either partially or entirely (fig.1.3).

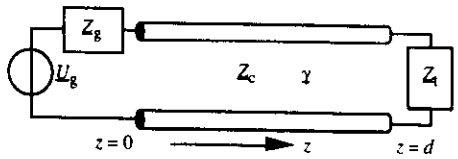

Fig. 1.3 Transmission line with generator and load

When the load does not absorb entirely the incoming signal the part that is not absorbed is reflected and travels back towards the generator. In turn the generator

absorbs part of the returned signal and reflects the remainder of it. As this doubly reflected signal reaches the load, part of it is reflected again, and the procedure is repeated indefinitely (fig. 1.4).

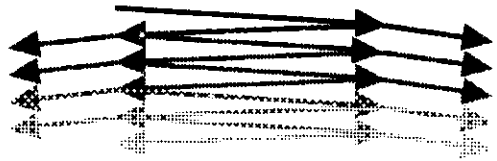

Fig. 1.4 Multiple reflections

This means that an infinite number of signals travel back and forth along the transmission line, creating a condition of *multiple reflections*. At any point along the transmission line, the composite forward wave results from the combination of the infinite series of all the successive forward waves while the composite reverse wave is the combination of all reverse waves. The signal levels thus depend on the characteristics of the generator and load, represented by their equivalent circuits.

Boundary conditions at the load

A linear load is considered, represented by its impedance $\underline{Z}_t$, and connected at the end of the line at $z = d$ (fig. 1.3). The voltage $\underline{U}_t$ across the load is the transmission line voltage, while the current $\underline{I}_t$ flowing across the load is the output current at the end of the line

$$\underline{U}_t = \underline{U}(d) \quad [\mathrm{V}] \qquad (1.11)$$

$$\underline{I}_t = \underline{I}(d) \quad [\mathrm{A}] \qquad (1.12)$$

Taking the ratio of the two quantities, the boundary condition for the local impedance at the end of the line is obtained

$$\underline{Z}(d) = \underline{Z}_t = \frac{\underline{U}(d)}{\underline{I}(d)} = \frac{\underline{U}_+ e^{-\underline{\gamma}d}\left[1+\underline{\rho}(d)\right]}{\underline{Y}_c \underline{U}_+ e^{-\underline{\gamma}d}\left[1-\underline{\rho}(d)\right]} = \underline{Z}_c \frac{1+\underline{\rho}(d)}{1-\underline{\rho}(d)} = \underline{Z}_c \frac{1+\underline{\rho}_t}{1-\underline{\rho}_t} \quad [\Omega] \qquad (1.13)$$

where $\underline{\rho}_t = \underline{\rho}(d)$ is the load's reflection factor. This expression provides a relationship for the two unknown constants $\underline{U}_+$ and $\underline{U}_-$. Generally, the ratio $\underline{U}_-/\underline{U}_+ = \underline{\rho}(0)$ is determined. The reflection factor along the line can now be expressed in terms of the load impedance

$$\underline{\rho}(z) = \underline{\rho}(0)e^{2\underline{\gamma}z} = \frac{\underline{Z}_t - \underline{Z}_c}{\underline{Z}_t + \underline{Z}_c} e^{2\underline{\gamma}(z-d)} \qquad [1] \tag{1.14}$$

The impedance at every point along the line $\underline{Z}(z)$ defined in (1.10) can also be determined in terms of the load impedance. Carrying out some simple calculations yields

$$\underline{Z}(z) = \underline{Z}_c \frac{1+\underline{\rho}(z)}{1-\underline{\rho}(z)} = \underline{Z}_c \frac{(\underline{Z}_t + \underline{Z}_c) + (\underline{Z}_t - \underline{Z}_c)e^{2\underline{\gamma}(z-d)}}{(\underline{Z}_t + \underline{Z}_c) - (\underline{Z}_t - \underline{Z}_c)e^{2\underline{\gamma}(z-d)}} = \underline{Z}_c \frac{\underline{Z}_t - \underline{Z}_c \tanh\left[\underline{\gamma}(z-d)\right]}{\underline{Z}_c - \underline{Z}_t \tanh\left[\underline{\gamma}(z-d)\right]}$$

$$[\Omega] \qquad (1.15)$$

and the impedance at the input of the line is simply obtained by letting $z = 0$

$$\underline{Z}_{in} = \underline{Z}(0) = \underline{Z}_c \frac{1+\underline{\rho}(0)}{1-\underline{\rho}(0)} = \underline{Z}_c \frac{\underline{Z}_t + \underline{Z}_c \tanh\left(\underline{\gamma}d\right)}{\underline{Z}_c + \underline{Z}_t \tanh\left(\underline{\gamma}d\right)} \qquad [\Omega] \tag{1.16}$$

Matched reflectionless termination

One particular termination presents a definite interest in practice, and that is the case where $\underline{Z}_t = \underline{Z}_c$. As can be seen in (1.14), one then has $\underline{\rho}_L = 0$, which implies that $\underline{U}_- = 0$, *i.e.* there is no backward wave. All the power carried by the forward wave is absorbed by the load, that is called a *matched* or *reflectionless* termination. The local impedance (1.15) is then everywhere equal to the characteristic impedance of the transmission line. A transmission line terminated by a reflectionless load is the ideal situation one generally wishes to obtain for high-frequency operation.

Short-circuit

The introduction of a perfectly conducting plane across the transmission line at $z = d$ imposes the boundary condition $\underline{U}(d) = 0$. This condition is satisfied when $\underline{Z}_t = 0$, and thus $\underline{\rho}_t = -1$. The reflection factor and the local impedance along the line then become

$$\underline{\rho}(z) = -e^{2\underline{\gamma}(z-d)} \qquad [1] \tag{1.17}$$

$$\underline{Z}(z) = -\underline{Z}_c \tanh\left[\underline{\gamma}(z-d)\right] \qquad [\Omega] \tag{1.18}$$

Open-ended transmission line

When the conductors of the transmission line end in the plane $z = d$ the boundary condition on the current requires that $\underline{I}(L) = 0$. This condition is satisfied when $\underline{Z}_t = \infty$ and thus $\underline{\rho}_t = 1$. The reflection factor and the local impedance along the line then become

$$\underline{\rho}(z) = e^{2\underline{\gamma}(z-d)} \qquad [1] \tag{1.19}$$

$$\underline{Z}(z) = -\underline{Z}_c \coth\left[\underline{\gamma}(z-d)\right] \qquad [\Omega] \tag{1.20}$$

Reactive terminations

More generally, any purely *reactive termination* cannot absorb any power. This only happens when the load impedance has no real component, *i.e.* when $\underline{Z}_t = jX_t$ and in the limiting cases $\underline{Z}_t = 0$ and $\underline{Z}_t = \infty$.

Remark

A short-circuit can be realized by introducing a sharp boundary, such that all field components vanish for $z \geq L$. For an open transmission line, on the other hand, the boundary only involves the current on the conductors, and some of the fields extend beyond the open end of the line's conductors at $z = L$. Some electrical energy is thus stored in the vicinity of the end of the line. Rather than an ideal open-circuit, one then has a capacitive termination. When the frequency is large enough, open-ended transmission lines also radiate part of the signal.

Computation of the input impedance

The impedance at the input of a transmission line is given by eqn.(1.11). The expressions contains hyperbolic functions of complex numbers, difficult and tedious to determine without the help of a computer. A software (**IP**) was developed for this very purpose for a calculator [1] and Ifor PC [2]. To obtain the input impedance to a circuit made with cascaded transmission lines, with series and shunt components, one answers questions put forth by the program. The load is specified, either by its impedance or by its admittance. The operator can connect a section of transmission line (defined by its characteristic impedance or admittance, propagation factor and length), a series or shunt connected component (defined either by its impedance or its admittance). The calculations then yield the input impedance to the assembly, and the process can be repeated any number of times — allowing thus to analyze quite complex structures.

Examples of Application

Question 1 : A load of impedance $Z_L = 200 - j\ 150\ \Omega$ is connected to a telephone line with a characteristic admittance $Y_c = 0.00156 + j\ 0.00144$ S. One wishes to know the input impedance at 1 kHz at a distance of 5 miles from the termination, the propagation factor being $\gamma = 0.1243 + j\ 0.1347$.

Answer 1 : These quantities are introduced into the program, and the result of the calculations is then displayed : $Z_{in} = 392.0681 - j\ 249.695\ \Omega$.

Question 2 : The operations that are traditionally made on the Smith chart [1] can similarly be made on the computer, following exactly the same sequence of operations (but here with lossy lines). An example outlined in [1] presents all the various situations which one might encounter (Fig. 1.5).

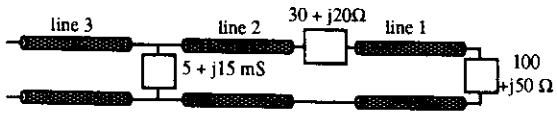

Figure 1.5 Assembly of lossy lines with series and shunt components

Three sections of lossy transmission lines, with different parameters, are connected with two complex impedances, one of them in series, the other one in shunt. The assembly is terminated by a complex load impedance. The input impedance to this assembly is to be found with the following parameters for the three sections of transmission lines

Line #	α Np/cm	β rad/cm	G_c Siemens	B_c Siemens	d cm
1	0.1	1.25	0.02	0.0016	2
2	0.05	1.5	0.05	0.00166	4
3	0.01	1.2	0.01	0.00008	10

Answer 2: Point **A** is simply the load impedance, $Z_L = 100 + j150\ \Omega$. The impedance at the input of the first section of line , at point **B**, is calculated on the computer, yielding :

$$Z_B = 27.437 + j\ 32.461$$

The next operation is the addition of the series impedance, giving at point **C** :

$$Z_C = 57.437 + j\ 52.461$$

This is the load impedance at the end of the second section of transmission line. The characteristic admittance is introduced in the program, and the input impedance to this section obtained :

$$Z_D = 24.327 + j\ 21.906$$

We now add a parallel admittance, which is simply done in the computer program, yielding:

$$Z_E = 34.7605 - j\ 6.82744$$

This is the load impedance terminating the third line section. The input impedance of the complete assembly is then obtained by cascading this section of line, yielding :

$$Z_F = 51.958 - j\ 41.348$$

Remark

By using this program, a rather complicated problem involving lossy lines, series and shunt connected elements was solved. The process parallels the use of the Smith chart, but is extended to a problem that cannot be solved simply on the Smith chart. This program may thus run a quick analysis of a transmission line layout and determine the effectiveness of some matching design or the sensitivity to one of its parameters. On the other hand, the procedure is still rather lengthy and it would take some time to analyze the response of a transmission line assembly over a broad range of frequencies or to optimize a design.

This program could also be incorporated into a more complete computing scheme, to provide data over a range of frequencies and parameters — because carrying out the complete sequence of computations for every case would tend to be lengthy and boring, and errors may well occur during the process.

Matching

The power transferred from a generator to a load depends on the generator, the load, and the connecting transmission line. At any given frequency, the maximum power transfer is obtained at the *conjugate match* when the impedance of the termination seen across the transmission line is the complex conjugate of the generator

impedance. Unfortunately, this condition is strongly dependent on phase shift and can only be satisfied over a narrow frequency range or with a short connecting line.

When the bandwidth requirements of the conjugate match are not satisfied, one must instead use the *reflectionless match*, in which reflections are reduced as much as possible. For high frequency applications, matching practically always implies reducing reflections, because requirements are specified in terms of a maximum reflection.

The presence of reflections is unwanted in most high frequency applications, as reflections produce bothersome echoes (fig. 1.4), locally increase the amplitude of the fields (which may cause breakdowns in high power systems) and detunes the signal generators. Therefore one of the most important parts in the design of any high frequency systems involves matching.

For the sake of completeness, one must also mention the existence of a third matching concept, used to provide the lowest possible noise figure when amplifying very small amplitude signals. In this case, one looks neither for the largest output power nor for the lowest reflection but the target is to maximize the signal-to-noise ratio.

By connecting reactive (lossless) elements and sections of transmission line in front of the load, one tries to bring the input impedance of the assembly as close as possible to the characteristic impedance of the line. One first assumes that lines are lossless and that purely reactive elements are used. The effect of losses in real elements is evaluated in a later section with CAD simulation programs [3].

Matching with Series Components

The insertion of series components within a transmission line is considered in program **IP** [2]: to obtain a reflectionless match, the input impedance must equal the characteristic impedance of the line. To obtain this result, a section of transmission line is inserted, with a length such that the real part of the input impedance is the characteristic impedance of the line. Reflectionless matching is then achieved by adding a reactance. Two possibilities exist (Fig. 1.6), one using an inductance, the other a capacitor. The program **IM** determines the electrical length d of the transmission line, given by

$$\tan\beta d = \frac{X_L Z_c \pm \sqrt{R_L Z_c\left[(R_L - Z_c)^2 + X_L^2\right]}}{|\underline{Z}_L|^2 - R_L Z_c} \qquad (1.21)$$

The $\pm$ sign indicates that there are two solutions, and one obtains in this manner the two line lengths d_1 and d_2. The reactance that must be connected is then given by the imaginary part of the input impedance calculated with eqn. (1.15).

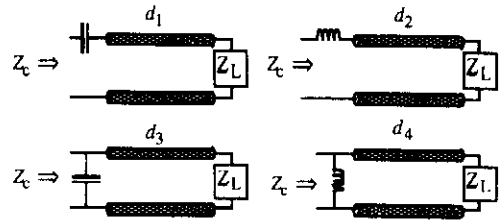

Figure 1.6 Matching with series or with shunt reactive elements

Matching with Shunt Components

The same approach is followed when matching with shunt elements, the transmission lines being related by $d_4 = d_1 \pm \lambda/4$, $d_3 = d_2 \pm \lambda/4$ (Fig. 1.6).

The computer program provides a large flexibility, as the load and the transmission line can be specified in terms of their impedances as well as their admittances. Distances are specified in "units of length" that may be selected arbitrarily — but must then be used consistently.

Shunt susceptances are often preferred to series reactances for matching because matching stubs are easily realized in many technologies. A capacitance is a short open-ended stub, while inductances are realized with short short-circuited stubs.

The developments given here consider matching with lossy lines and purely reactive (lossless) components. When losses are present in either the line or the matching elements, the computations become more complex: the effect of losses can be evaluated with program **IP**.

Perfect matching conditions can only be achieved at a single frequency, because the phase-shift provided by the section of the line and the shunt susceptance (or the series reactance) are both frequency dependent. This means that reflections will increase as one moves away from the design frequency.

Example of Application

Question: we wish to match a load impedance $\underline{Z}_L = 127 + j22\ \Omega$ to a transmission line having a characteristic admittance $Y_c = 0{,}023$ S, considering the four possible approaches, shunt and series, capacitive and inductive reactances, and compare the length requirements for all of them. The wavelength is $\lambda = 10$ cm.

Answer: Introducing the values in the program **IM** readily provides the four desired responses as follows

	Length of line	Reactance
Series inductance	0.8967 cm	49.3708 Ω
Series capacitance	4.2186 cm	–49.3708 Ω
Shunt inductance	1.7186 cm	–38.2890 Ω
Shunt capacitance	3.3967 cm	38.289 Ω

For this particular situation, matching with inductances requires shorter sections of line, the shortest one being for a series inductance. The best choice depends, obviously, on the parameters of the load. More information about matching techniques can be found in several books [3-6]

Quarter-Wave Transformer

One can also match with a single section of transmission line of characteristic impedance Z_x in front of the termination. This technique is generally used to match resistive terminations and also to make transitions between different transmission lines, in which cases the load impedance is purely real $Z_L = R_L$ (Fig. 1.7).

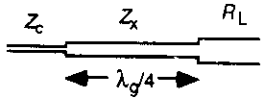

Figure 1.7 Matching with a quarter-wave transformer.

The transformer section is a quarter of a guided wavelength ($\lambda_g/4$) long, and its characteristic impedance is the geometrical mean of the impedances on its two sides:

$$Z_x = \sqrt{Z_c R_L} \tag{1.22}$$

Unfortunately, the transformer can only be a quarter wavelength long at a single frequency, which is its design frequency f_0. Its matching properties progressively degrade as frequency changes. Therefore, the band over which the quarter-wave transformer can effectively match a load is limited. Matching over a broader frequency ranges requires multiple section transformers. The width and length of successive sections are adjusted in such a way that the reflections at successive steps tend to cancel out not at a single frequency but at several frequencies within the band of operation.

Broadband Matching

The matching processes are frequency-limited because all elements have a frequency-dependent behavior. Matching over broader frequency bands is achieved with multistage configurations, which provide a larger number of parameters. Calculations become involved, and require computer optimization techniques [3].

The optimization scheme generally used is sketched in Figure 4.18, which shows the main steps of the computer optimization process. First, the operator introduces the impedance of the termination that is to be matched and defines the input impedance that should be achieved (frequency range and maximum reflection tolerated). A configuration for the matching structure should also be provided, indicating where reactive elements and transmission line sections can be placed. Some approximate values should be provided for the matching elements, to be used as a starting point for the optimization process carried out by the computer [7].

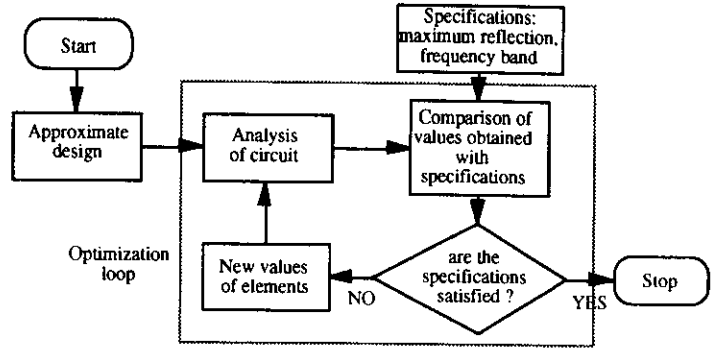

Figure 1.8 Optimization process used for broadband matching.

The computer analyzes the circuit built with the approximate values, it determines its input impedance over the specified frequency range and compares it with the specified requirements. When the specifications are met, the process stops. When not satisfied, parameter values are modified and the new circuit is analyzed.

In the *gradient search*, parameters are slightly modified one after the other and the new results carefully monitored, trying to reach a minimum. The process is repeated either until the desired requirement is satisfied or over a specified number of cycles,. If the process does not converge, this means that the configuration selected is not adequate and another one must be chosen. The matching process is physically limited:

for instance, one cannot match a high-Q cavity over a wide bandwidth (at least, not when using lossless components only). The matching structure may also become too cumbersome and may not fit within the available space.

Matching optimization processes do not always converge toward the most favorable situation because one might encounter local minima. Also, one may not have any approximate values to start the optimization process. Another approach selects the matching components at random (*Monte Carlo process*) within specified ranges. The result obtained is compared to the previous one and the best of the two is retained. The random approach does not converge in a regular fashion.

It is often interesting to combine the two approaches to reach an optimal situation. The stochastic approach determines the general area in which the optimum could be located, and the gradient search pinpoints its actual position.

REFERENCES :

[1] Gardiol, F.E., *Lossy Transmission Lines*, Norwood: Artech House, 1987.

[2] Gardiol, F.E., *LOSLIN: Lossy Line Calculations Software and User's Manual*, Norwood: Artech House, 1989.

[3] Abric, P.L., *The Design of Impedance-Matching Networks for Radio-Frequency and Microwave Amplifiers*, Norwood, MA: Artech House, 1986.

[4] Chen, Wai-Kai, *Theory and Design of Broadband Matching Networks*. Oxford: Pergamon, 1976.

[5] Matthaei, G., Young, L., and Jones, E.M.T., *Microwave Filters, Impedance Matching Networks and Coupling Structures*. New York: McGraw Hill, 1964.

[6] Thomas, R.L., *A Practical Introduction to Impedance Matching*. Norwood, MA: Artech House, 1976.

[7] Dobrowolski, J.A., *Introduction to Computer Methods for Microwave Circuit Analysis and Design*, Norwood, MA: Artech House, 1991.

Annex: Transmission Line Software (in FORTRAN 77)

```
      implicit real*8(a-h,o-z)
120   call clear
      print*, '          LOSSY TRANSMISSION LINES '
      print*, '          SELECTION  ICTP COURSE '
      print*
      print*, 'By Fred E. Gardiol, Professor, LEMA'
      print*, 'Laboratoire d''Electromagnetisme et d''Acoustique'
      print*, 'Ecole Polytechnique Federale, ELB-Ecublens'
      print*, 'CH-1015 LAUSANNE, Switzerland'
      print*
      print*, 'This software is a complement to'
      print*, 'the book "Lossy Transmission Lines" published '
      print*, 'by ARTECH HOUSE, Inc. in 1987'
      print*
      print*, '1  Microstrip '
      print*, '2  Input Impedance '
      print*, '3  Reactive Matching '
      print*, '4  Transformers '
      print*
      print*, 'Punch the number next to the desired program '
      read*, ivar
      print*
      go to (136,161,171,172)ivar

136   print*
      call MS
      print*
      go to 100

161   print*
      call IP
      print*
      go to 100

171   print*
      call RM
      print*
      go to 100

172   print*
      call TM
      print*
      go to 100
```

```
100   print*
      print*
      print*, 'Do you want to use another program?  yes = 1 '
      read*, in
      if(in.eq.1) go to 120
      stop
      end

      subroutine IP
      complex gammal,Z,ZC,ZP,ZS,egl,th
301   call clear
      print*,' INPUT IMPEDANCE'
      print*
      print*, 'The  program IP determines the impedance at the input'
      print*, 'of an assembly of cascaded transmission line segments'
      print*, 'shunt and series impedances, connected to a load'
      print*, 'impedance or admittance'

      print*, 'NOTE : the unit of length can be chosen arbitrarily'
      print*, 'as long as it is used consistently'
      print*
      print*, 'impedances are in OHMS '
      print*, 'admittances are in SIEMENS'
      print*

      print*, 'if you want to introduce a load impedance, punch 1'
      print*, 'if you want to introduce a load admittance, punch 2 '
      read*,in
      if(in.eq.1) go to 302
      if(in.ne.2) go to 307
      print*

      print*,'enter the real part of the load admittance '
      read*, GL
      print*,'enter the imaginary part of the load admittance '
      read*, BBL
      Z = cmplx(1.,0.)/cmplx(GL,BBL)
      go to 303

302   print*,'enter the real part of the load impedance '
      read*,  RL
      print*,'enter the imaginary part of the load impedance '
      read*, XL
      Z = cmplx(RL,XL)

303   print*, 'if you want to connect'
      print*, '      - a section of transmission line,'
      print*, '        in terms of line impedance,     punch 1'
```



```
      print*, '      - a section of transmission line,'
      print*, '        in terms of line admittance     punch 2 '
      print*, '      - a series-connected impedance,   punch 3'
      print*, '      - a series-connected admittance,  punch 4'
      print*, '      - a shunt connected impedance,    punch 5'
      print*, '      - a shunt connected admittance,   punch 6 '
      read*,ivar
      go to (304,305,306,307,308,309) ivar
      go to 311

304   print*,'enter the real part of the line impedance '
      read*,  RC
      print*,'enter the imaginary part of the line impedance '
      read*, XC
      ZC = cmplx(RC,XC)
      go to 312

305   print*,'enter the real part of the line admittance '
      read*,  GC
      print*,'enter the imaginary part of the line admittance '
      read*, BC
      ZC = cmplx(1.,0.)/cmplx(GC,BC)

312   print*,'enter the attenuation per unit length alpha '
      read*,  alpha
      print*,'enter the phaseshift per unit length beta '
      read*, beta
      print*, 'enter the length of the transmission line section '
      read*, TRL
      gammal = cmplx(alpha*2*TRL,beta*2*TRL)
      egl = cexp(gammal)
      th = (egl-cmplx(1.,0.))/(egl+cmplx(1.,0.))
      Z = ZC*(Z+ZC*th)/(ZC+Z*th)
      go to 310

306   print*,'enter the real part of the series impedance '
      read*,  RS
      print*,'enter the imaginary part of the series impedance '
      read*, XS
      Z = Z + cmplx(RS,XS)
      go to 310

307   print*,'enter the real part of the series admittance '
      read*, GS
      print*,'enter the imaginary part of the series admittance '
      read*, BBS
      ZS = cmplx(1.,0.)/cmplx(GS,BBS)
      Z = Z + ZS
```

```
      go to 310

308   print*,'enter the real part of the shunt impedance '
      read*,  RP
      print*,'enter the imaginary part of the shunt impedance '
      read*, XP
      ZP = cmplx(RP,XP)
      Z = (ZP*Z)/(ZP + Z)
      go to 310

309   print*,'enter the real p .rt of the shunt admittance '
      read*,  GP
      print*,'enter the imaginary part of the shunt admittance '
      read*, BP
      ZP = cmplx(1.,0.)/cmplx(GP,BP)
      Z = (ZP*Z)/(ZP + Z)
      go to 310

310   print*
      write(6,123)Z
123   format(2x,'input impedance = ',f9.4,' +j ',f9.4,'  ohms',/)

      print*
      print*,'do you want to add another element ?'
      print*,'if yes, punch 1     if no, punch 0 '
      read*,in
      if(in.eq.1) go to 303
      print*

311   print*,'do you want to analyze another case ?'
      print*,'if yes, punch 1     if no, punch 0 '
      read*,in
      if(in.eq.1) go to 301
      return
      end

      subroutine MS
304   call clear
      print*, 'MICROSTRIP LINE'

      print*
      print*, 'The program MS,  based on equations (3.102-3.106)'
      print*, 'calculates the characteristic impedance, the'
      print*, 'wavelength and the attenuation of a microstrip line,'
      print*, 'made of a thin flat conductor deposited on top of a'
      print*, 'metal-backed dielectric substrate.'
```



```
      print*
      print*,'enter strip width w in millimetres '
      read*,ww
      print*,'enter strip thickness  b in millimetres '
      read*,b

      print*,'enter substrate thickness  h in mm. '
      read*,h
      print*,'enter relative permittivity epsilon '
      read*,eps
      print*, 'enter dielectric loss tangent tand '
      read*,tand

      x = h
      if((ww.lt.h/6.283)) x = 6.28319*ww
      w = ww + (b/3.14159)*(1 + log(2*x/b))

      print*,'lower end of the frequency band in GHz ? '
      read*,fmin
      print*,'upper end of the frequency band in GHz ? '
      read*,fmax
      print*,'frequency step, in GHz ? '
      read*,df

      call clear
      write(6,100)

100   format(  ' MICROSTRIP LINE',/)

      write(6,122)ww,h,b,eps,tand
122   format(2x,'w = ',f7.3,' h = ',f7.3,' b = ',f9.5,
     X  ' eps r = ',f7.3,' tan d = ',f9.5,/)
      write(6,101)
101   format(7x,'f',6x,'eff eps',5x,'wl',7x,'Zc',8x,'att')
      write(6,102)
102   format(5x,'GHz',18x,'mm',6x,'ohms',7x,'dB/m',/)

      nf = 1
      if(df.gt.1d-5) nf = (fmax - fmin + 0.00001)/df + 1

      do 153 if = 1,nf
      f = if-1
      f = fmin + f*df

      e1 = (eps + 1)/2
      e2 = ((eps - 1)/2)/(1 + 12*h/w)**0.5
      eeo = e1 + e2
      if(w.lt.h) eeo = eeo + ((eps -1)/2)*0.04*((1-w/h)**2)
```

```
      if(w.lt.h) zo = 59.94*log((8*h/w)+(w/(4*h)))
      if(w.ge.h) zo = 376.6/((w/h)+1.393+0.667*log((w/h)
     X  + 1.444))

      z = zo/sqrt(eeo)

      do 152 i = 1,20
      fd = z/(2.513274*h)
      G = 0.6 + 0.009*z
      ee =  eps - (eps - eeo)/(1 + G*(f/fd)**2)
      z = zo/sqrt(ee)
  152 continue

      wl = 299.7925/(f*sqrt(ee))
      a = 27.3*((ee-1.)/(eps-1.))*(eps/ee)*(tand/(wl*1d-3))
      a = a + 8.686*8.240996*sqrt(f)/(w*z)

      write(6,123)f,ee,wl,z,a
  123 format(5(2x,f8.3))

  153 continue

      print*
      print*,'do you want to analyse another case ?'
      print*,'if yes, punch 1     if no, punch 0 '
      read*,in
      if(in.eq.1) go to 304
      continue
      return
      end

      subroutine RM
      complex ZL,XJ,ZIN
      XJ = cmplx(0.,1.)
  301 call clear
      print*,'REACTIVE MATCHING'
      print*
      print*, 'The  program RM determines : '
      print*
      print*, '  the length of transmission line to be placed '
      print*, '  in front of the load and the value of the reactive'
      print*, '  element that must be connected, either in series'
      print*, '  or in parallel, to provide a reflectionless match.'
      print*, '  (section 7.2)'
      print*

      print*, 'if you want to introduce a load impedance, punch 1'
      print*, 'if you want to introduce a load admittance, punch 2 '
```



```
      read*,in
      print*
      go to (302,303)in
      go to 304

  303 print*,'enter the real part of the load admittance '
      read*, GL
      print*,'enter the imaginary part of the load admittance '
      read*, BBL
      RL = GL/(GL**2 + BBL**2)
      XL = -BBL/(GL**2 + BBL**2)
      go to 305

  302 print*,'enter the real part of the load impedance '
      read*,  RL
      print*,'enter the imaginary part of the load impedance '
      read*, XL

  305 ZL = cmplx(RL,XL)
      print*
      print*, 'if you want to specify the line impedance, punch 1'
      print*, 'if you want to specify the line admittance, punch 2 '
      read*,in
      print*
      go to (306,307)in
      go to 304

  307 print*,'enter the line admittance '
      read*,  GC
      ZC = 1./GC
      go to 308

  306 print*,'enter the line impedance '
      read*,  ZC

  308 print*
      print*,'enter the wavelength (in arbitrarily chosen units) '
      read*, wl

      beta = 6.2831853/wl
      print*

      p = sqrt(RL*ZC*((RL-ZC)**2 + XL**2))
      d = XL**2 + RL**2 - ZC*RL

      A = (ZC*XL + p)/d
      ZIN = cmplx(ZC,0.)*(ZL + cmplx(ZC*A,0.))/
     >      (cmplx(ZC,0.) + ZL*cmplx(0.,A))
```

```
      XM = aimag(ZIN)
      if (XM.ge.0.) d2 = (1./beta)*atan(A)
      if (XM.lt.0.) d1 = (1./beta)*atan(A)

      B = (ZC*XL - p)/d
      ZIN = cmplx(ZC,0.)*(ZL + cmplx(0.,ZC*B))/
     >     (cmplx(ZC,0.) + ZL*cmplx(0.,B))
      XM = aimag(ZIN)
      if (XM.ge.0.)d2 = (1./beta)*atan(B)
      if (XM.lt.0.)d1 = (1./beta)*atan(B)

      if (XM.lt.0.) XM = - XM

      if (d1.lt.0.) d1 = d1 + 3.14159/beta
      if (d2.lt.0.) d2 = d2 + 3.14159/beta
      d3 = d2  + 0.5*3.14159/beta
      d4 = d1  + 0.5*3.14159/beta

      if (d3*beta.gt.3.14159) d3 = d3 - 3.14159/beta
      if (d4*beta.gt.3.14159) d4 = d4 - 3.14159/beta

      print*, 'to use a series inductance, punch 1'
      print*, 'to use a series capacitance, punch 2'
      print*, 'to use a shunt inductance, punch 3'
      print*, 'to use a shunt capacitance, punch 4 '
      read*, ic
      go to (309,310,311,312)ic
      go to 304

  309 call clear
      write(6,124)
  124 format(//,' MATCHING WITH SERIES INDUCTANCE',/)
      write(6,196)ZL,ZC
  196 format(2x,'ZL = ',f10.5,' + j ',f10.5,/,
     X '  ZC = ',f10.5,/)

      write(6,128)d1

      write(6,129)XM
      go to 304

  310 call clear
      write(6,125)
  125 format(//,' MATCHING WITH SERIES CAPACITANCE',/)
      write(6,196)ZL,ZC
      write(6,128)d2
      write(6,129)XM
      go to 304
```



```
  311 call clear
      write(6,126)
  126 format(//,' MATCHING WITH SHUNT INDUCTANCE',/)
      write(6,196)ZL,ZC
      XM = ZC**2/XM
      write(6,128)d3
      write(6,130)XM
      go to 304


  312 call clear
      write(6,127)
  127 format(//,' MATCHING WITH SHUNT CAPACITANCE',/)
      write(6,196)ZL,ZC
      XM = ZC**2/XM
      write(6,128)d4
      write(6,130)XM

  128 format(2x,'length of trm. line = ',f12.4,' length units')
  129 format(2x,'series reactance  = ',f12.4,' ohms')
  130 format(2x,'shunt reactance  = ',f12.4,' ohms')

  304 print*
      print*,'do you want to match another load ?'
      print*,'if yes, punch 1     if no, punch 0 '
      read*,in
      if(in.eq.1) go to 301
      return
      end

      subroutine TM
      complex ZL,XJ,ZIN
      XJ = cmplx(0.,1.)
  301 call clear
      print*,'TRANSFORMER  MATCHING'
      print*
      print*, 'The  program TM determines : '
      print*
      print*, '- in the case of a quarter wave transformer, '
      print*, '  the length of transmission line to be placed '
      print*, '  in front of the load and the characteristic'
      print*, '  impedance of the quarter wave section (sec. 7.3.1)'
      print*
      print*, '- in the case of the generalized transformer,'
      print*, '  the length and the characteristic impedance'
      print*, '  of the transformer section (sec. 7.3.2)'
      print*
```

```
      print*, 'if you want to introduce a load impedance,  punch 1'
      print*, 'if you want to introduce a load admittance, punch 2 '
      read*,in
      print*
      go to (302,303)in
      go to 304

303   print*,'enter the real part of the load admittance '
      read*, GL
      print*,'enter the imaginary part of the load admittance '
      read*, BBL
      RL = GL/(GL**2 + BBL**2)
      XL = -BBL/(GL**2 + BBL**2)
      go to 305

302   print*,'enter the real part of the load impedance '
      read*,  RL
      print*,'enter the imaginary part of the load impedance '
      read*, XL

305   ZL = cmplx(RL,XL)

      print*
      print*, 'if you want to specify the line impedance,  punch 1'
      print*, 'if you want to specify the line admittance, punch 2 '
      read*,in
      print*
      go to (306,307)in
      go to 304

307   print*,'enter the line admittance '
      read*,  GC
      ZC = 1./GC
      go to 308

306   print*,'enter the line impedance '
      read*,  ZC

308   print*
      print*,'enter the wavelength (in arbitrary length units) '
      read*, wl
      beta = 6.2831853/wl
      print*

      ZIN = RL
      d = 0.
      XA = abs(xl)
```



```
      if(XA.lt.1.d-9)go to 312

      print*, 'to use a quarter wave transformer, punch 1'
      print*, 'to use a generalized transformer,  punch 2 '
      read*, ic
      go to (309,310)ic
      go to 304

309   call clear
      write(6,124)
124   format(//,' MATCHING WITH QUARTER WAVE TRANSFORMER',/)

      p = ZC**2 - RL**2 - XL**2
      d = sqrt(p**2 + 4*(XL**2)*ZC**2)
      A = (p + d)/(2*XL*ZC)
      B = (p - d)/(2*XL*ZC)

      AA = (1./beta)*atan(A)
      BB = (1./beta)*atan(B)

      if(aa.lt.0) go to 311
      ZIN = cmplx(ZC,0.)*(ZL + cmplx(0.,ZC*A))/
     >       (cmplx(ZC,0.)+ZL*cmplx(0.,A))

      d = aa
      go to 312

311   ZIN = cmplx(ZC,0.)*(ZL + cmplx(ZC*B))/
     >    (cmplx(ZC,0.) + ZL*cmplx(0.,B))
      d = bb

312   ZX = sqrt(dble(ZIN)*ZC)

      wl4 = wl/4.
      write(6,195)ZL,ZC
195   format(2x,'ZL = ',f10.5,' + j ',f10.5,/,
     X  '  ZC = ',f10.5,/)

      if(XA.gt.1.d-9)write(6,126)d
126   format(2x,'transmission line length = ',d10.3,' length units')
      write(6,127)ZX
127   format(2x,'characteristic impedance = ',d8.3,' ohms')
      write(6,128)wl4
      go to 304

315   write(6,130)
130   format(2x,'there is no solution for this set of parameters',/)
      go to 304
```

```
310   call clear
      write(6,125)
125   format(//,' MATCHING WITH GENERALIZED TRANSFORMER',/)

      V = ZC*RL + XL**2/(RL/ZC - 1.)
      if (V.lt.0.) go to 315
      ZX = sqrt(V)
      d = (1./beta)*atan((ZX/XL)*(1-RL/ZC))
      if(d.lt.0.) d = d + 3.14159/beta
      write(6,195)ZL,ZC

      write(6,128)d
128   format(2x,'length of transformer = ',d10.3,' length units')
      write(6,129)ZX
129   format(2x,'characteristic impedance = ',d8.3,' ohms')
      go to 304
304   print*
      print*,'do you want to match another load ?'

      print*,'if yes, punch 1     if no, punch 0 '
      read*,in
      if(in.eq.1) go to 301
      return
      end

      subroutine clear
      character i,j,k,l
      i=char(27)
      j=char(91)
      k=char(ichar('2'))
      l=char(74)
      write(*,*)i,j,k,l
      return
      end
```


FINITE DIFFERENCES IN THE TIME DOMAIN (FDTD)

Introduction

Finite differences in time domain (FDTD) provide an approximate "full wave" solution to Maxwell's equations. It has been used in many electromagnetic problems, including: scattering and radar cross-section (RCS) calculations, electromagnetic pulse penetration problems, transients, inverse problems, and recently, planar microstrip circuit and antenna problems. With current advances in computer technology (i.e. memory, speed, graphical interfaces, massively parallel processing), FDTD becomes a serious approach to solve complex electromagnetic problems. Some of its more salient features include the ability to handle various types of discontinuities (even time-dependent ones) within the resolution of the FDTD mesh and the ability to solve transient problems. The method can also provide frequency-domain information with the use of a Fourier transform and can solve both "closed" and, with the addition of absorbing boundaries, "open" problems.

The FDTD method was first presented to the electromagnetics community by Yee in 1966 [2.1]. In his paper, Yee solved the transient scattering of a cylinder in two dimensions. Maxwell's equations were solved by using the central difference approximation for both the partial space and time derivatives and incorporating the appropriate boundary conditions in a "leapfrog" algorithm. In this algorithm both space and time are discretized and the solution is obtained by "marching" in time. It should be noted that other finite difference schemes can be used to solve time-dependent Maxwell's equations. For example, algorithms which have been used to solve the time-dependent equations of fluid dynamics have been successfully employed [2.28].

Principle of the method

The method is briefly outlined in this section to provide a general understanding of its basic principles. To show how the technique works, the FDTD algorithm is applied to the time-dependent source-free Maxwell's curl equations in free space — the approach can also be extended to consider more complex media with various boundary conditions.

$$\mu \frac{\partial \mathbf{H}(t,\mathbf{r})}{\partial t} = -\nabla \times \mathbf{E}(t,\mathbf{r}) \qquad \varepsilon \frac{\partial \mathbf{E}(t,\mathbf{r})}{\partial t} = \nabla \times \mathbf{H}(t,\mathbf{r}) \tag{2.1}$$

The curl operations yield ix scalar partial derivative equations, which become in the rectangular coordinate system

$$\mu\frac{\partial H_x}{\partial t} = \frac{\partial E_y}{\partial z} - \frac{\partial E_z}{\partial y} \qquad \mu\frac{\partial H_y}{\partial t} = \frac{\partial E_z}{\partial x} - \frac{\partial E_x}{\partial z} \qquad \mu\frac{\partial H_z}{\partial t} = \frac{\partial E_x}{\partial y} - \frac{\partial E_y}{\partial x}$$

$$\varepsilon\frac{\partial E_x}{\partial t} = \frac{\partial H_z}{\partial y} - \frac{\partial H_y}{\partial z} \qquad \varepsilon\frac{\partial E_y}{\partial t} = \frac{\partial H_x}{\partial z} - \frac{\partial H_z}{\partial x} \qquad \varepsilon\frac{\partial E_z}{\partial t} = \frac{\partial H_y}{\partial x} - \frac{\partial H_x}{\partial y} \tag{2.2}$$

Similar expressions can be obtained in other coordinate systems, but they are considerably more complex, so that the FDTD approach usually considers square of cubic discretization schemes. Space is divided into cubic cells like the one shown in figure 2.1.

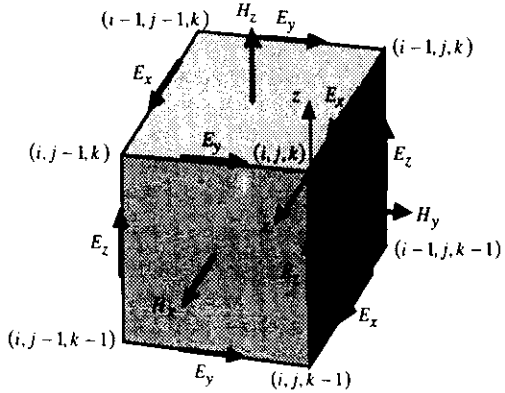

Figure 2.1 Yee's FDTD mesh.

The time and spatial derivatives are then approximated by central differences, i.e. the partial derivatives are replaced by finite differences in time and space. The two expressions on the left in eqn. (2.2) then take the form of eqn. (2.3)

In eqn. (2.3) the electric field and the magnetic field are calculated on alternate time steps and depend only on information obtained in the previous time step. Similarly, the central difference approximation is used for the remaining four equations. The indices (i, j, k) denote position and the index (n) denotes the time step. The quantities Δx, Δy, and Δz are the physical distances between nodes in the i, j, and k directions respectively.

Usually one takes $\Delta x = \Delta y = \Delta z$ for all nodes, so that the FDTD mesh is cubic. Non cubic mesh configurations have also been investigated.

$$\frac{H_x^{n+\frac{1}{2}}\left(i, j+\frac{1}{2}, k+\frac{1}{2}\right) - H_x^{n-\frac{1}{2}}\left(i, j+\frac{1}{2}, k+\frac{1}{2}\right)}{\Delta t} =$$

$$\frac{E_y^n\left(i, j+\frac{1}{2}, k+1\right) - E_y^n\left(i, j+\frac{1}{2}, k\right)}{\mu\,\Delta z} - \frac{E_z^n\left(i, j+1, k+\frac{1}{2}\right) - E_z^n\left(i, j, k+\frac{1}{2}\right)}{\mu\,\Delta y}$$

$$\frac{E_x^n\left(i+\frac{1}{2}, j, k\right) - E_x^{n-1}\left(i+\frac{1}{2}, j, k\right)}{\Delta t} =$$

$$\frac{H_z^{n-\frac{1}{2}}\left(i+\frac{1}{2}, j+\frac{1}{2}, k\right) - H_z^{n-\frac{1}{2}}\left(i+\frac{1}{2}, j-\frac{1}{2}, k\right)}{\varepsilon\,\Delta y} - \frac{H_y^{n-\frac{1}{2}}\left(i+\frac{1}{2}, j, k+\frac{1}{2}\right) - H_x^{n-\frac{1}{2}}\left(i+\frac{1}{2}, j, k-\frac{1}{2}\right)}{\varepsilon\,\Delta z} \tag{2.3}$$

More detailed discussions can be found in a large number of references [2..9, 2.21, 2.27]. We consider first the time dependent, source free, differential Maxwell's equations in free space:

Time is stepped (or marched) in Δt intervals, but again, however, deviations may occur in particular situations. To insure the stability of the method, Taflove [2.3] has established a relationship between distances between nodes and the time step size. The following condition must be satisfied:

$$v_{\max}\Delta t \le \frac{1}{\sqrt{(\Delta x)^{-2} + (\Delta y)^{-2} + (\Delta z)^{-2}}} \tag{2.4}$$

where $v_{\max}$ is the maximum phase velocity.

Resolution of the problem

The structure to be analyzed is first discretized by an FDTD mesh. If it is an "open" problem (where the structure is residing in an infinite medium) the mesh must still remain finite. This implies that some kind of boundary condition must be applied on the sides of the mesh to simulate an infinite medium, so that an outward traveling wave that encounters the mesh boundary is not reflected. In the situation of a "closed" problem, such as a closed cavity, the mesh is terminated on the cavity boundary.

Initially, all the field quantities are set equal to zero. An excitation is provided at some input points to the mesh. These input points could form a plane in front of an

object (as in a scattering problem), some sort of prescribed field distribution under a microstrip line or in a coaxial cross section. The excitation is a function of time. A Gaussian pulse is often used, with parameters selected to cover a desired frequency spectrum. After the initial injection of the pulse into the mesh, time is stepped until all field quantities return to zero.

A time harmonic function, discretized in time, is used to perform narrow band analysis. In this case, time is stepped until all field quantities vary in a time harmonic manner. This may take several complete frequency cycles, depending on the quality factor (Q) of the structure [2.4].

Output data are determined at some observation point(s), where the desired field components are recorded as a function of time. If transient information is required, no further processing of the data is needed. On the other hand, frequency-domain information is obtained by performing a Fourier transform on the response function.

Applications

Initial activities in FDTD centered around scattering and penetration problems. Three years after Yee's pioneering paper, FDTD was used to solve scattering in a time varying inhomogeneous medium [2.2]. Following these two publications, FDTD lay dormant, at least in the open literature, until the mid-1970's. Probably the reason for this resting period was the fact that FDTD requires vast amounts of memory and computational time. By the mid-1970's, computer memory had advanced to the point where FDTD could be utilized. Taflove and his co-workers applied FDTD to scattering of 2-D dielectric circular cylinders [2.3] and the scattering of 2-D PEC square and circular cylinders [2.12]. Three dimensional (3-D) FDTD was used to predict the transient response of a F-111 aircraft [2.5, 2.6] and the scattering of other electrically large structures [2.16].

Penetration studies are also well represented in FDTD literature. Electromagnetic coupling into complex cavities [2.11], heavily shielded cavities [2.13], cylindrical "missile-like" cavities [2.7], lossy dielectic spheres [2.8], and even missile guidance sections [2.10] have been analyzed using FDTD. In addition, induced currents on wires placed in the interior of cavities have also been calculated [2.22].

In "open" problems, such as scattering and penetration problems, the mesh must be terminated by appropriate absorbing boundary conditions (ABCs). These boundary conditions have been the subject of investigations [2.9, 2.36]. It was noted that frequency domain data derived from the time domain by means of a Fourier transform are "very sensitive to numerical errors, notably those resulting from the imperfect

treatment of the absorbing boundary conditions" [2.23]. FDTD numerical experiments involving varying the distance of the absorbing boundary from the scatterer led Kriegsmann et. al. to formulate an "on-surface radiation condition" (OSRC) [2.20]. For a certain class of geometries, this technique collapses the absorbing condition on the surface of the scatterer.

It was only recently that FDTD was used to analyze more "traditional" microwave structures. Gwarek used FDTD to solve arbitrarily shaped 2-D microwave circuits [2.17, 2.24]. Choi and Hoefer applied FDTD to determine the eigenvalues of various dielectrically loaded cavities, a fin line in a cavity, and microstrip in a cavity [2.18]. Characteristics of microstrip lines, discontinuities, hybrids, and bends have been the subject of many recent publications [2.23, 2.25, 2.26, 2.33, 2.35, 2.37]. Slotlines and coplanar waveguides have also been investigated [2.32]. Even microstrip patch antennas have been analyzed successfully [2.31, 2.37, 2.42].

Effect of dispersion

Fundamentally, the FDTD method assumes that the properties of the media under study are frequency-independent. In reality, however, real materials have frequency-dependent characteristics, in particular when they exhibit losses. In several technical journals an open question was addressed to time domain experts, asking how frequency-dependent characteristics of materials could be taken into account in an FDTD analysis [2.29, 2.30]. An interesting approach was put forward by Luebbers et. al. [2.38]. In their method, frequency information of the material is Fourier transformed to a time domain function and is incorporated into the FDTD formulation.

Computation Requirements

Efforts to improve the modeling of structures, to reduce memory requirements and execution time have been and will continue to be active areas of research. FDTD algorithms were also derived in generalized curvilinear coordinates [2.14, 2.34] and spherical coordinates [2.15]. Utilization of these techniques circumvent errors which are introduced by the "staircase" approximations required when employing rectangular grids. In addition, non-uniform grids in rectangular coordinates have been studied [2.39, 2.41]. The structure can be divided in fine grids in areas where the fields change rapidly, while a coarse grid is used in the remaining part of the structure, thus saving memory space. Computational savings were also obtained by including edge singularities directly in the FDTD algorithm [2.40].

Sufficiently large computer resources are now available, and a fair amount of experience has been gained by many users of FDTD. More complex structures, such as printed circuits inside of n enclosure, are the subject of current investigations. FDTD is not restricted to rectangular enclosures, in contrast to some integral and waveguide methods. FDTD offers enough flexibility to model three dimensional circuits residing an arbitrary shaped three dimensional cavities (within the resolution of the mesh!).

Of course, like any other method, FDTD also presents drawbacks. The first and foremost problem is that of computer memory. A very large number of cells is required to model an electrically large three dimensional structure. Each cell requires 6 real memory locations, one for each field component. As individual field components do not share the same spatial coordinates, interfaces and boundaries may be inadequately defined, which ultimately degrades the solution. It was feared that the excitation of microstrip circuits could not be handled properly. However, it was recently demonstrated that coaxial excitations [2.42] can be successfully modeled.

References

[2.1] Yee, K. S., "Numerical solution of initial boundary value problems involving Maxwell's equations in isotropic media," *IEEE Trans. Antennas Propagat.*, vol. AP-14, no. 3, pp. 302-307, May 1966.

[2.2] Taylor, C. D., Lam, D.-H., and Shumpert, T. H., "Electromagnetic pulse scattering in time-varying inhomogeneous media," *IEEE Trans. Antennas Propagat.*, vol. AP-17, no. 5, pp. 585-589, Sept. 1969.

[2.3] Taflove, A. and Brodwin, M. E., "Numerical solution of steady-state electromagnetic scattering problems using the time-dependent Maxwell's equations," *IEEE Trans. Microwave Theory Tech.*, vol. MTT-23, no. 8, pp. 623-630, Aug. 1975.

[2.4] Taflove, A., and Brodwin, M. E., "Computation of the electromagnetic fields and induced temperatures within a model of the microwave-irradiated human eye," *IEEE Trans. Microwave Theory Tech.*, vol. MTT-23, no. 11, pp. 888-896, Nov. 1975.

[2.5] Kunz, K. S. and Lee, K.-M., "A three-dimensional finite-difference solution of the external response of an aircraft to a complex transient EM environment: Part I – The method and its implementation," *IEEE Transactions on Electromagnetic Compatibility*, vol. EMC-20, no. 2, pp. 328-333, May 1978.

[2.6] Kunz, K. S. and Lee, K-M, "A three-dimensional finite-difference solution of the external response of an aircraft to a complex transient EM environment: Part II – Comparison of predictions and measurements," *IEEE Transactions on Electromagnetic Compatibility*, vol. EMC-20, no. 2, pp. 333-341, May 1978.

[2.7] Taflove, A., "Application of the finite-difference time-domain method to sinusoidal steady-state electromagnetic-penetration problems," *IEEE Transactions on Electromagnetic Compatibility*, vol. EMC-22, no. 3, pp. 191-202, Aug. 1980.

[2.8] Holland, R., Simpson, L., and Kunz, K. S., "Finite-difference analysis of EMP coupling to lossy dielectric structures," *IEEE Transactions on Electromagnetic Compatibility*, vol. EMC-22, no. 3, pp. 203-209, Aug. 1980.

[2.9] Mur, G., "Absorbing boundary conditions for the finite-difference approximation of the time-domain electromagnetic-field equations," *IEEE Transactions on Electromagnetic Compatibility*, vol. EMC-23, no. 4, pp. 377-382, Nov. 1981.

[2.10] Taflove, A. and Umashankar, K., "A hybrid moment method/finite-difference time-domain approach to electromagnetic coupling and aperture penetration into complex geometries," *IEEE Trans. Antennas Propagat.*, vol. AP-30, no. 4, pp. 617-627, July 1982.

[2.11] Merewether, D. E. and Fisher, R., "Finite-difference Analysis of EM fields inside complex cavities driven by large apertures," *IEEE Transactions on Electromagnetic Compatibility*, vol. EMC-24, no. 4, pp. 406-410, Nov. 1982.

[2.12] Umashankar, K. and Taflove, A., "A novel method to analyze electromagnetic scattering of complex objects," *IEEE Transactions on Electromagnetic Compatibility*, vol. EMC-24, no. 4, pp. 397-405, Nov. 1982.

[2.13] Holland, R. and Williams, J. W., "Total-field versus scattered-field finite-difference codes: a comparative assessment," *IEEE Transactions on Nuclear Science*, vol. NS-30, no. 6, pp. 4583-4588, Dec. 1983.

[2.14] Holland, R., "Finite-difference solution of Maxwell's equations in generalized non orthogonal coordinates," *IEEE Transactions on Nuclear Science*, vol. NS-30, no. 6, pp. 4589-4591, Dec. 1983.

[2.15] Holland, R., "THREDS: A finite-difference time-domain EMP code in 3d spherical coordinates," *IEEE Transactions on Nuclear Science*, vol. NS-30, no. 6, pp. 4592-4595, Dec. 1983.

[2.16] Taflove, A., Umashankar, K. R., and Jurgens, T. G., "Validation of FD-TD modeling of the radar cross section of three-dimensional structures spanning up to nine wavelengths," *IEEE Trans. Antennas Propagat.*, vol. AP-33, no. 6, pp. 662-666, June 1985.

[2.17] Gwarek, W. K., "Analysis of an arbitrarily-shaped planar circuit–a time-domain approach," *IEEE Trans. Microwave Theory Tech.*, vol. MTT-33, no. 10, pp. 1067-1072, Oct. 1985.

[2.18] Choi, D. H. and Hoefer, W. J. R., "The finite-difference–time-domain method and its application to eigenvalue problems," *IEEE Trans. Microwave Theory Tech.*, vol. MTT-34, no. 12, pp. 1464-1470, Dec. 1986.

[2.19] Taflove, A. and Umashankar, K. R., "The finite-difference time-domain (FD-TD) method for electromagnetic scattering and interaction problems," *Journal of Electromagnetic Waves and Applications*, vol. 1, no. 3, pp. 244-267, 1987.

[2.20] Kriegsmann, G. A., Taflove, A., and Umashankar, K. R., "A new formulation of electromagnetic wave scattering using an on-surface radiation boundary condition approach," *IEEE Trans. Antennas Propagat.*, vol. AP-35, no. 2, pp. 153-161, Feb. 1987.

[2.21] Cangellaris, A. C., Lin, C., and Mei, K. K., "Point-matched time domain finite element methods for electromagnetic radiation and scattering," *IEEE Trans. Antennas Propagat.*, vol. AP-35, no. 10, pp. 1160-1173, Oct. 1987.

[2.22] Umashankar, K. R., Taflove, A., and Beker, B., "Calculation and experimental validation of induced currents on coupled wires in an arbitrary shaped cavity," *IEEE Trans. Antennas Propagat.*, vol. AP-35, no. 11, pp. 1248-1257, Nov. 1987.

[2.23] Zhang, X., Fang, J., Mei, K. K., and Liu, Y., "Calculations of the dispersive characteristics of microstrips by the time-domain finite difference method," *IEEE Trans. Microwave Theory Tech.*, vol. 36, no. 2, pp. 263-267, Feb. 1988.

[2.24] Gwarek, W. K., "Analysis of arbitrarily shaped two-dimensional microwave circuits by finite-difference time-domain," *IEEE Trans. Microwave Theory Tech.*, vol. 36, no. 4, pp. 738-744, April 1988.

[2.25] Zhang, X. and Mei, K. K., "Time-domain finite difference approach to the calculation of the frequency-dependent characteristics of microstrip discontinuities," *IEEE Trans. Microwave Theory Tech.*, vol. 36, no. 12, pp. 1775-1787, Dec. 1988.

[2.26] Zhang, X. and Mei, K. K., "Time-domain finite difference approach for the calculation of microstrip open-circuit end effect," *1988 IEEE MTT-S Digest*, pp. 363-366.

[2.27] Taflove, A. and Umashankar, K. R., "Review of FD-TD numerical modeling of electromagnetic wave scattering and radar cross section," *Proceedings of the IEEE*, vol. 77, no. 5, pp. 682-699, May 1989.

[2.28] Shankar, V., Hall, W. F., and Mohammadian, A. H., "A time-domain differential solver for electromagnetic scattering problems," *Proceedings of the IEEE*, vol. 77, no. 5, pp. 709-721, May 1989.

[2.29] Gardiol, F., "Comments about time domain techniques in electromagnetics," *IEEE Antennas and Propagation Society Newsletter*, pp. 36-37, Aug. 1989.

[2.30] Gardiol, F., "Comments about time domain techniques in electromagnetics," *IEEE MTT-S Newsletter*, pp. 43-44, Summer/Fall 1989.

[2.31] Reineix, A. and Jecko, B., "Analysis of microstrip patch antennas using finite difference time domain method," *IEEE Trans. Antennas Propagat.*, vol. 37, no. 11, pp. 1361-1369, Nov. 1989.

[2.32] Liang, G.-C., Liu, Y.-W., and Mei, K. K., "Full-wave analysis of coplanar waveguide and slotline using the time-domain finite-difference method," *IEEE Trans. Microwave Theory Tech.*, vol. 37, no. 12, pp. 1949-1957, Dec. 1989.

[2.33] Railton, C. J. and McGeehan, J. P., "Analysis of microstrip discontinuities using the finite difference time domain technique," *1989 IEEE MTT-S Digest*, pp. 1009-1012.

[2.34] Fusco, M., "FDTD algorithm in curvilinear coordinates," *IEEE Trans. Antennas Propagat.*, vol. 38, no. 1, pp. 76-89, Jan. 1990.

[2.35] Moore, J. and Ling, H., "Characterization of a 90° microstrip bend with arbitrary miter via the time-domain finite difference method," *IEEE Trans. Microwave Theory Tech.*, vol. 38, no. 4, pp. 405-410, April 1990.

[2.36] Canning, F. X., "On the application of some radiation boundary conditions," *IEEE Trans. Antennas Propagat.*, vol. 38, no. 5, pp. 740-745, May 1990.

[2.37] Sheen, D. M., Ali, S. M., Abouzahra, M. D., and Kong, J. A., "Application of the three-dimensional finite-difference time-domain method to the analysis of planar microstrip circuits," *IEEE Trans. Microwave Theory Tech.*, vol. 38, no. 7, pp. 849-857, July 1990.

[2.38] Luebbers, R., Hunsberger, F. P., Kunz, K. S., Standler, R. B., and Schneider, M., "A frequency-dependent finite-difference time-domain formulation for dispersive materials," *IEEE Transactions on Electromagnetic Compatibility*, vol. EMC-32, no. 3, pp. 222-227, Aug. 1990.

[2.39] Railton, C. J. and McGeehan, J. P., "An analysis of microstrip with rectangular and trapezoidal conductor cross sections," *IEEE Trans. Microwave Theory Tech.*, vol. 38, no. 8, pp. 1017-1022, Aug. 1990.

[2.40] Shorthouse, D. B. and Railton, C. J., "Incorporation of static singularities into finite difference time domain technique with application to microstrip structures," *20th European Microwave Conference*, pp. 531-536.

[2.41] Railton, C. J. and McGeehan, J. P., "Characterization of discontinuities in microstrip with rectangular and trapezoidal cross-section," *20th European Microwave Conference*, pp. 549-554, 1990.

[2.42] Wu, C., Wu, K.-L., Bi, Z., and Litva, J., "Modeling of coaxial-fed microstrip patch antenna by finite difference time domain method," *Electronics Letters*, vol. 27, no. 19, pp. 1691-1692, 12 Sept. 1991.

VARIATIONAL PRINCIPLES : FINITE ELEMENTS

Introduction

The finite element method (FEM) is a powerful analysis technique that was originally used by the civil and mechanical engineering community to solve problems of structures, heat transfer, mass transfer, elasticity, and fluid mechanics. Cross fertilization between engineering disciplines took place, and FEM also began to be utilized in electrical engineering problems around the late 1960's, to calculate propagation constants of dielectrically loaded metallic waveguides with an arbitrarily cross section. Since then, FEM has been constantly refined for electrical engineering problems as evidenced by the large number of papers on the subject.

The FEM is usually concerned with finding solutions to Maxwell's equations within finite volumes. Consider a vector field within a volume which is enclosed by a surface, in figure 3.1. In order to obtain a unique vector field, both the curl and the divergence of the field must be defined at every point within the volume, and both the normal and tangential components of the field must be defined on the surface enclosing the volume.

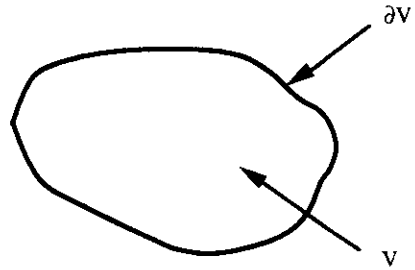

Figure 3.1 Volume V enclosed by surface ∂V.

The goal of the FEM is to determine a unique vector field satisfying Maxwell's equations for given geometry and boundary conditions.

Variational Principle

The fundamental principles of the FEM are presented here — more detailed explanations can be found in the many publications devoted to this topic (for instance [3.14, 3.17, 3.24, 3.34]). The FEM for electromagnetic problems requires a description of the geometry, Maxwell's equations and appropriate boundary conditions. Maxwell's equations in time harmonic form in a medium with permittivity ε and permeability μ are given, in complex notation, by

$$\nabla \times \underline{\mathbf{E}}(\mathbf{r}) = -j\omega\mu\underline{\mathbf{H}}(\mathbf{r}) \qquad \nabla \cdot \underline{\mathbf{E}}(\mathbf{r}) = 0$$
$$\nabla \times \underline{\mathbf{H}}(\mathbf{r}) = j\omega\varepsilon\underline{\mathbf{E}}(\mathbf{r}) \qquad \nabla \cdot \underline{\mathbf{H}}(\mathbf{r}) = 0 \tag{3.1}$$

where $\underline{\mathbf{E}}(\mathbf{r})$ and $\underline{\mathbf{H}}(\mathbf{r})$ are respectively the electric and the magnetic phasor-vectors (complex vector quantities) and there are no free charges. For complex structures — inhomogeneous media or oddly-shaped boundaries — these equations cannot be solved analytically and an alternate approach is based on a variational expression. As an example, a variational formulation for the magnetic field for three dimensional problems is given here:

$$F(\underline{\mathbf{H}}) = \int_V \left[\frac{1}{\varepsilon}(\nabla \times \underline{\mathbf{H}}) \cdot (\nabla \times \underline{\mathbf{H}}^*) - \omega^2 \mu \underline{\mathbf{H}} \cdot \underline{\mathbf{H}}^* \right] dV \tag{3.2}$$

Equation (3.2) is stationary with respect to perturbations about the true magnetic field solution and can be related to the stored energy.

Triangular division

Once a variational form has been obtained, the entire surface or volume is divided into finite elements. These finite elements may, for example, be triangles in the case of a surface, or tetrahedrons in the case of a volume (Figure 3.2).

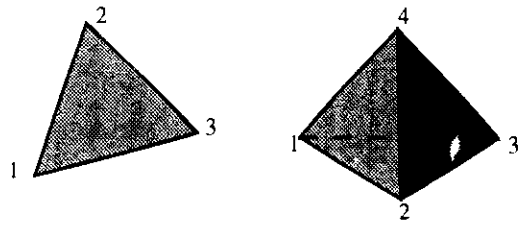

Figure 3.2 Some simple finite elements: the triangle for surfaces and the tetrahedron for volumes.

The field is then expressed by algebraic functions whose domain of support is over a single finite element. The functional is then minimized with respect to the algebraic functions. This produces a sparsely populated matrix. When dealing with a large number of unknowns, special sparse matrix solvers can be employed, saving considerable amounts of memory and CPU time.

Survey of Applications

The early papers on FEM mainly concentrated on the solution of waveguide problems. Formulations were first given for waveguides with arbitrary cross sections and dielectric fillings [3.1]. Silvester provided numerical results when he solved for the cutoff frequencies for T-septate and vaned rectangular waveguides [3.2]. Then, examples of rectangular waveguides that were partially filled with dielectric began to appear in the literature [3.3, 3.5]. These canonical problems were of particular interest because results could be checked against analytic solutions. Modal behavior of what is essentially shielded microstrip lines were investigated by several researchers [3.4, 3.5, 3.6]. A practical example of a dissipative surface waveguide was studied when a guiding structure consisting of a railroad track with a dielectric insert was investigated [3.10]. In addition, different algebraic functions were considered to approximate the field over a finite element [3.9].

Until this point, however, FEM formulation was in terms of longitudinal field components (Ez, Hz). Konrad gave a general three component vector variational formulation [3.8] which opened the way for true vector three dimensional problems. Although some attempts to solve three dimensional problems were made prior to the general three component vector formulation [3.7], these were limited in scope because of the their scalar formulation.

Attention began to shift toward three dimensional problems. Dielectrically loaded cavities were studied by using tetrahedrons as the finite elements [3.11]. In addition to solving dielectrically loaded cavities, Webb, Maile, and Ferrari presented scattering by simple three dimensional objects in waveguides [3.13]. Cavities with circular symmetry, such as a linear accelerator cavity, were investigated by Davies et. el. [3.12]. However, it soon became apparent that the FEM formulation was plagued by serious problems. In the case of longitudinal field formulation these problems were mathematical singularities. In the case of vector formulation these problems were "spurious solutions". These spurious solutions would be found to be mixed and interlaced among the true physical solutions.

Since the mid 1980's the majority of FEM papers in the literature have dealt almost exclusively with this problem of spurious solutions. It is interesting to note that in his original paper on the vector variational formulation, Konrad recognized the existence of spurious solutions and suggested rigorous enforcement of the boundary conditions to eliminate them. However, it was reported that this attempt was not adequate. Many different methods have been suggested to eliminate spurious solutions. Some of these suggestions include: the use of a penalty function to enforce a divergenceless field [3.15, 3.19], the use of divergence-free fields to expand the field [3.22], forcing the solution of the FEM to be non-divergent [3.31], the use of special finite elements [3.16, 3.21], methods to confine the spurious solutions to a particular frequency range [3.18, 3.20], the use of discrimination techniques to separate "real" from "spurious" solutions [3.25], FEM formulation in terms of all six field components [3.32], modifications to the governing vector equations [3.36], and the use of tangential finite elements [3.26, 3.38] (previous finite elements were "nodal" finite elements).

FEM has been used in the quasi-TEM analysis of transmission lines. Pantic and Mittra employed a variational formulation which was based on Poisson's equation and also incorporated singular and infinite elements in their analysis [3.23]. Skin-effects in quasi-TEM analysis have also been accounted for [3.27]. Singular elements have been used in modeling waveguides which have "sharp metal edges" [3.30, 3.37], dielectric waveguides have been investigated using infinite elements [3.33] and efficient methods employing hermitic polynomials have been used in solving rectangular and ridged waveguide problems [3.28]. In an interesting approach, Csendes and Lee combined the planar waveguide model of microstrip circuits and the "transfinite element method" to predict the performance of several practical MMIC structures [3.29].

Scattering produced by three dimensional obstacles in waveguides have been investigated by Ise, Inoue, and Koshiba. In their first approach, they employed tetrahedral finite elements and a penalty function to eliminate spurious solutions [3.35]. Their second approach used rectangular parallelepipedic edge elements [3.39].

Recently, Hewlett-Packard has released a software package named the "High-Frequency Structure Simulator" (HFSS), which was developed at Anasoft Corporation [3.40]. HFSS can find scattering parameters and field distributions of enclosed three dimensional passive microwave circuits. HFSS uses FEM to model these complicated three dimensional structures. HFSS possesses advanced solid modeling capabilities and post data processing.

However, as with most general purpose codes, accurate results are obtained at the expense of memory and CPU time. A specific approach aimed at and optimized for a particular class of problems should be more computationally efficient.

A final word should be said about the so-called boundary element method (BEM). Many authors present it as a version of FEM. Although specialized to problems defined on surfaces [3.41], it has also been claimed that it reduces to an integral equation approach combined with the method of moments [3.42]. Additional evidence reduces BEM to field related principles combined with a generalized mode-matching method has also been presented [3.43].

Example of application to an electrostatic problem

To illustrate the basic principle of the FEM, we consider here the resolution of Laplace's equation, which is encountered in electrostatic and magnetostatic problems, as well as in the determination of the transverse dependence of the fields in TEM transmission lines. The potential Φ is a solution of the equation

$$\nabla^2\Phi = 0 \tag{3.3}$$

The variational principle derived from eqn. (3.3) is in this case

$$F(\Phi) = \int_V |\nabla\Phi|^2 \, dV \tag{3.4}$$

The unknown potential Φ within each triangular region (two-dimensional case) with corners P, Q and R (figure 3.3) is approximated by a polynomial expansion in terms of the coordinates x y and z. A first order polynomial provides the simplest possible choice

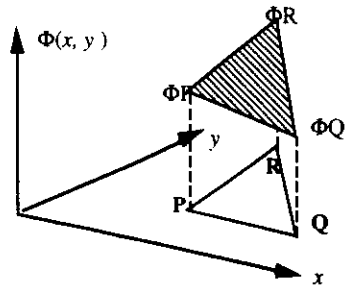

Figure 3.3 Polynomial approximation on a triangle

$$\Phi(x, y) = Lx + My + N \tag{3.5}$$

The coefficients L, M and N are directly related to the potentials on the three corners of the triangle. The first two terms are :

$$L = \frac{\Phi_P(y_Q - y_R) + \Phi_Q(y_R - y_P) + \Phi_R(y_P - y_Q)}{x_P(y_Q - y_R) + x_Q(y_R - y_P) + x_R(y_P - y_Q)}$$

$$M = \frac{\Phi_P(x_Q - x_R) + \Phi_Q(x_R - x_P) + \Phi_R(x_P - x_Q)}{y_P(x_Q - x_R) + y_Q(x_R - x_P) + y_R(x_P - x_Q)} \tag{3.6}$$

The value of N is not determined, because this parameter does not appear in later developments. The contribution of this particular triangle to the function $F(\Phi)$ in eqn.(3.4) is then given by

$$(L^2 + M^2) S_{PQR} \tag{3.7}$$

where S_{PQR} is the area of the triangle. Summing the contributions of all the triangles within the cross-section yields an approximation for $F(\Phi)$ that is a function of the potentials Φ_I at the corners of all the triangles. Since the smallest possible value for this function must be determined, its derivative with respect to every one of the Φ_Js is set equal to zero

$$\frac{\partial F(\Phi_A, \Phi_B, \ldots, \Phi_Z)}{\partial \Phi_J} = 0 \tag{3.8}$$

This provides a system of N linear equations with N unknowns, N being the number of corners of triangles not located on a metal boundary. Since the potential at any one point appears only within the expressions from the triangles adjacent to this point, the corresponding matrix is sparse. The system may be solved by matrix inversion or other suitable algorithms.

References

[3.1] Ahmed, S., "Finite-element method for waveguide problems," *Electronics Letters*, vol. 4, no. 18, pp. 387-389, 6 September 1968.

[3.2] Silvester, P., "A general high-order finite-element waveguide analysis program," *IEEE Trans. Microwave Theory Tech.*, vol. MTT-17, no. 4, pp. 204-210, April 1969.

[3.3] Ahmed, S. and Daly, P., "Finite-element methods for inhomogeneous waveguides," *IEE Proc.*, vol. 116, no. 10, pp. 1203-1208, October 1969.

[3.4] Daly, P., "Finite-element coupling matrices," *Electronics Letters*, vol. 5, no. 24, pp. 613-615, 27 November 1969.

[3.5] Csendes, Z. J. and Silvester, P., "Numerical solution of dielectric loaded waveguides: I-Finite-element analysis," *IEEE Trans. Microwave Theory Tech.*, vol. MTT-18, no. 12, pp. 1124-1131, December 1970.

[3.6] Daly, P., "Hybrid-mode analysis of microstrip by finite-element methods," *IEEE Trans. Microwave Theory Tech.*, vol. MTT-19, no. 1, pp. 19-25, January 1971.

[3.7] Silvester, P., "Tetrahedral polynomial finite elements for the Helmholtz equation," *Int. J. Numerical Meth. in Eng.*, vol. 4, pp. 405-413, 1972.

[3.8] Konrad, A., "Vector variational formulation of electromagnetic fields in anisotropic media," *IEEE Trans. Microwave Theory Tech.*, vol. MTT-24, no. 9, pp. 553-559, September 1976.

[3.9] Konrad, A., "Higher-order triangular finite elements for electromagnetic waves in anisotropic media," *IEEE Trans. Microwave Theory Tech.*, vol. MTT-25, no. 5, pp. 353-360, May 1977.

[3.10] McAulay, A. D., "Variational finite-element solution for dissipative waveguides and transport application," *IEEE Trans. Microwave Theory Tech.*, vol. MTT-25, no. 5, pp. 382-392, May 1977.

[3.11] Ferrari, R. L. and Maile, G. L., "Three-dimensional finite-element method for solving electromagnetic problems," *Electronics Letters*, vol. 14, no. 15, pp. 467-468, 20 July 1978.

[3.12] Davies, J. B., Fernandez, F. A., and Philippou, G., Y., "Finite element analysis of all modes in cavities with circular symmetry," *IEEE Trans. Microwave Theory Tech.*, vol. MTT-30, no. 11, pp. 1975-1980, November 1982.

[3.13] Webb, J. P., Maile, G. L., and Ferrari, R. L., "Finite-element solution of three-dimensional electromagnetic problems," *IEE Proc.*, vol. 130, pt. H, no. 2, pp. 153-159, March 1983.

[3.14] Silvester, P. P. and Ferrari, R. L., *Finite Elements for Electrical Engineers*. Cambridge, U. K.: Cambridge University Press, 1983.

[3.15] Rahman, B. M. A. and Davies, J. B., "Penalty function improvement of waveguide solution by finite elements," *IEEE Trans. Microwave Theory Tech.*, vol. MTT-32, no. 8, pp. 922-928, August 1984.

[3.16] Hano, M., "Finite-element analysis of dielectric-loaded waveguides," *IEEE Trans. Microwave Theory Tech.*, vol. MTT-32, no. 10, pp. 1275-1279, October 1984.

[3.17] Reddy, J. N., *An Introduction to the Finite Element Method.* New York: McGraw-Hill Book Company, 1984.

[3.18] Koshiba, M., Hayata, K., and Suzuki, M., "Improved finite-element formulation in terms of the magnetic field vector for dielectric waveguides," *IEEE Trans. Microwave Theory Tech.*, vol. MTT-33, no. 3, pp. 227-233, March 1985.

[3.19] Webb, J. P., "The finite-element method for finding modes of dielectric-loaded cavities," *IEEE Trans. Microwave Theory Tech.*, vol. MTT-33, no. 7, pp. 635-639, July 1985.

[3.20] Koshiba, M., Hayata, K., and Suzuki, M., "Finite-element formulation in terms of the electric-field vector for electromagnetic waveguide problems," *IEEE Trans. Microwave Theory Tech.*, vol. MTT-33, no. 10, pp. 900-905, October 1985.

[3.21] Konrad, A., "A direct three-dimensional finite element method for the solution of electromagnetic fields in cavities," *IEEE Trans. Magnetics*, vol. MAG-21, no. 6, pp. 2276-2279, November 1985.

[3.22] Kobelansky, A. J. and Webb, J. P., "Eliminating spurious modes in finite-element waveguide problems by using divergence-free fields," *Electronics Letters*, vol. 22, no. 11, pp. 569-570, 22 May 1986.

[3.23] Pantic, Z. and Mittra, R., "Quasi-TEM analysis of microwave transmission lines by the finite-element method," *IEEE Trans. Microwave Theory Tech.*, vol. MTT-34, no. 11, pp. 1096-1103, November 1986.

[3.24] Davies, A. J., *The Finite Element Method: A First Approach.* New York: Oxford University Press, 1986.

[3.25] Angkaew, T., Matsuhara, M., and Kumagai, N., "Finite-element analysis of waveguide modes: A novel approach that eliminates spurious modes," *IEEE Trans. Microwave Theory Tech.*, vol. MTT-35, no. 2, pp. 117-123, February, 1987.

[3.26] Barton, M. L. and Csendes, Z. J., "New vector finite elements for three dimensional magnetic field computation," *J. Appl. Phys.*, vol. 61, no. 8, pp. 3919-3921, 15 April 1987.

[3.27] Costache, G. I., "Finite element method applied to skin-effect problems in strip transmission lines," *IEEE Trans. Microwave Theory Tech.*, vol. MTT-35, no. 11, pp. 1009-1013, November 1987.

[3.28] Miniowitz, R. and Israel, M., "An efficient finite element method for non convex waveguide based on hermitian polynomials," *IEEE Trans. Microwave Theory Tech.*, vol. MTT-35, no. 11, pp. 1019-1026, November 1987.

[3.29] Csendes, Z. J. and Lee, J.-F., "The transfinite element method for modeling MMIC devices," *IEEE Trans. Microwave Theory Tech.*, vol. 36, no. 12, pp. 1639-1649, December 1988.

[3.30] Webb, J. P., "Finite element analysis of dispersion in waveguides with sharp metal edges," *IEEE Trans. Microwave Theory Tech.*, vol. 36, no. 12, pp. 1819-1824, December 1988.

[3.31] Konrad, A., "A method for rendering 3D finite element vector field solutions non-divergent," *IEEE Trans. Magnetics*, vol. MAG-25, no. 4, pp. 2822-2824, July 1989.

[3.32] Svedin, J. A. M., "A numerically efficient finite-element formulation for the general waveguide problem without spurious modes," *IEEE Trans. Microwave Theory Tech.*, vol. 37, no. 11, pp. 1708-1715, November 1989.

[3.33] McDougall, M. J. and Webb, J. P., "Infinite elements for the analysis of open dielectric waveguides," *IEEE Trans. Microwave Theory Tech.*, vol. 37, no. 11, pp. 1724-1731, November 1989.

[3.34] Davies, J. B., "The finite element method," Chapter 2 in *Numerical Techniques for Microwave and Millimeter-Wave Passive Structures*, edited by T. Itoh, New York, 1989, John Wiley and Sons, pp. 33-132.

[3.35] Ise, K., Inoue, K., and Koshiba, M., "Three-dimensional finite-element solution of dielectric scattering obstacles in a rectangular waveguide," *IEEE Trans. Microwave Theory Tech.*, vol. 38, no. 9, pp. 1352-1359, September 1990.

[3.36] Paulsen, K. D. and Lynch, D. R., "Elimination of vector parasites in finite element Maxwell solutions," *IEEE Trans. Microwave Theory Tech.*, vol. 39, no. 3, pp. 395-404, March 1991.

[3.37] Schiff, B., "Eigenvalues for ridged and other waveguides containing corners of angle 3p/2 or 2p by the finite element method," *IEEE Trans. Microwave Theory Tech.*, vol. 39, no. 6, pp. 1034-1039, June 1991.

[3.38] Lee, J.-F., Sun, D.-K., and Csendes, Z. J., "Full-wave analysis of dielectric waveguides using tangential vector finite elements," *IEEE Trans. Microwave Theory Tech.*, vol. 39, no. 8, pp. 1262-1271, August 1991.

[3.39] Kazuhire, K. I. and Koshiba, M., "Three-dimensional finite-element method with edge elements for electromagnetic waveguide discontinuities," *IEEE Trans. Microwave Theory Tech.*, vol. 39, no. 8, pp. 1289-1295, August 1991.

[3.40] Csendes, Z. J., "Finite element modeling of microwave and mm. wave discontinuities," presented at the International Workshop of the German IEEE/AP Chapter *CAD Oriented Numerical Techniques for the Analysis of Microwave and MM-Wave Transmission-Line Discontinuities and Junctions*, Stuttgart, Germany, September 13, 1991.

[3.41] Kagami, S. and Fukai, I., "Application of boundary-element method to electromagnetic field problems," *IEEE Trans. Microwave Theory Tech.*, vol. MTT-32, no. 4, pp. 455-461, April 1984.

[3.42] Morita, N., "Comments on 'Application of boundary-element method to electromagnetic field problems'," *IEEE Trans. Microwave Theory Tech.*, vol. MTT-33, no. 4, pp. 346-347, April 1985.

[3.43] Collin, R. E. and Ksienski, D. A., "Boundary element method for dielectric resonators and waveguides," *Radio Science*, vol. 22, no. 7, pp. 1155-1167, December 1987.

ANTENNAS AND ARRAYS

Definitions

Antennas are devices that provide a transition between a guided wave — traveling along a transmission line or in a waveguide — and a radiated wave, traveling in free unbounded space. There are many ways to make transitions, and therefore many kinds of antennas. The simplest one is just a piece of metallic wire, called a dipole. Flat metal plates also radiate, in a direction perpendicular to their surface (patch antennas).

Open waveguides can radiate directly into space (apertures). Their radiation characteristics can however be significantly enhanced by providing a tapered section which ensures a smooth transition from the waveguide to free space, making a horn (there are shape similarities between electromagnetics and acoustics).

All antennas radiate waves towards some preferential directions in space. They may be more or less "directive" depending on their symmetry and their dimensions, as compared to a wavelength of the signal. Dipoles possess a cylindrical symmetry and therefore their radiation is independent of the azimuthal coordinate. The radiation is however dependent on the elevation, decreasing to zero on the axis of the dipole. Horns generally direct the wave in the direction perpendicular to their opening.

The half-power beamwidth (3-dB) α of an antenna generally meets the following requirement:

$$\alpha \geq \lambda / D \quad \text{[radians]} \tag{4.1}$$

where D is the "major" dimension of the antenna and $\lambda = c_0 / f$ is the signal wavelength. This means that a small antenna cannot provide a narrow beam. When one wishes to obtain a narrow beam while keeping the antenna size reasonable, one must use small wavelengths, and thus high frequency signals. This requirement is particularly important for radars, and led to the development of the field of microwaves, and more recently to the expansion within the millimeter wave region.

For broadcasting and mobile telephones, every point at ground level should receive the signal, in this case broad (or ominidirectional) beams are required and low directivity (small) antennas are used.

In most other communication links, on the contrary, one wishes to transmit a signal from a transmitter to one single specific receiver — but not to flood the surrounding countryside. Narrow beams are then required, so that high-directivity antennas must be used. It is important to guarantee the confidentiality of communica-

tions — a hot topic! A signal reaching a wrong receiver may also perturb the reception of the latter, in particular if the perturbing signal has a large amplitude. By concentrating the energy of the signal into a narrow beam and pointing it in the right direction, the power required to ensure the transmission is reduced. By reciprocity, the same holds true for the receiving antenna, which should only receive signal from a small region of space, in which the transmitter is located.

Simple metal antennas like dipoles and patches radiate most efficiently at or near of a resonance, when their size D is approximately equal to a half wavelength ($\lambda/2$). The beamwidth is then about two radians, very wide, and such an antenna has a very small directivity: it is suitable for broadcasting, but not communication links.

There are two ways to make high-directivity antennas with low directivity radiating elements:

- by combining the radiating element with a focusing device in the same manner as is done in telescopes for lightwaves. Mirrors and lenses are used for this purpose: for antennas, parabolic reflectors are most often used (dishes).
- by combining the signals radiated by several elements in such a way that the waves add up in the direction of the link and cancel each other out in the other directions. The assembly of radiating elements is called an array.

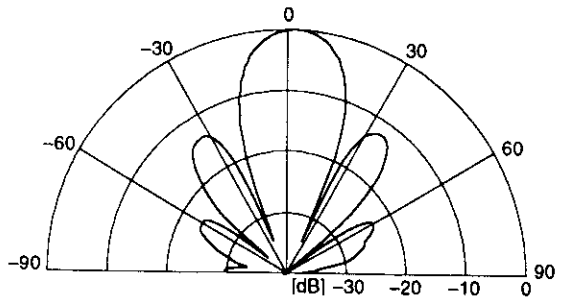

Figure 4.1 Radiation pattern of an antenna array, showing main beam and sidelobes

The radiation of an antenna occurs mostly in a "main beam" in which most of the power of the signal is concentrated (Fig. 4.1). It is surrounded by sidelobes, which result from the incomplete canceling of the signal in the other directions. Sidelobes are generally unwanted, and the main task in antenna design is the reduction of sidelobe amplitude. As a rule, if the antenna size remains the same, any reduction of the sidelobe level also widens the main beam.

ANTENNA DESIGN USING PERSONAL COMPUTERS

Software packages were developed and are commercially available. As an example, the following sections are based on the softwares developed by Professor David Powar at the University of Massachusetts (Amherst) and published by Artech House in 1985 under the title above. This set of programs is user-friendly and deals with most usual types of antennas. It is particularly useful to provide a general understanding of the basic characteristics of antennas, providing gain, beamwidth and, in some cases, antenna patterns. As pointed out by the author, however, simple approximations were used for some developments, to ensure that suitable responses would be obtained in a reasonable time on a personal computer. For more accurate computations, the use of a more powerful mainframe computer would be advisable.

The book contains 19 programs, grouped in 4 chapters

GENERAL APPLICATIONS

TLINE — Transmission Line Design

This program calculates the characteristic impedance and the attenuation of coaxial lines, two-wire lines, microstrips and striplines, for geometrical dimensions and material properties specified by the user. Both the dielectric and the conductor losses are taken into account. For microstrips and striplines, the dimensions necessary to obtain a specified impedance are also determined.

DIRECT — Directivity Calculations

This program determines the maximum directivity of an arbitrary antenna pattern, specified by the product of an element factor by an array factor. The number of array elements, their spacing and the phaseshifts between adjacent elements determine the array factor. The elements can be chosen as isotropic radiators (omnidirectional), short dipoles (placed collinear or parallel to each other) and half wave dipoles. The user can also define other patterns by entering a user-defined function. The program carries out the numerical integration of the pattern and determines the maximum directivity. The user selects the number of integration points and can thus check the convergence.

LINE — Line Source Patterns

The radiation pattern of an electric line source of arbitrary length L (fig. 4.2) is determined and plotted in polar coordinates, indicating the main beam position and the 3-dB beamwidth. Five distributions of the current on the wire can be considered:

uniform, triangular, cosine, cosine squared and cosine on a pedestal. It is possible in this manner to see how the pattern changes with the current distribution and the length of the radiating line.

Figure 4.2 Line source

FRIIS — Link Calculations

This program performs communication link calculations, including the losses resulting from impedance and polarization mismatches. The power received is calculated as a function of the power fed to the transmitting antenna, the gains and mismatches of the two antennas, the range and the frequency. The polarization mismatch is determined by introducing the axial ratios of the antennas and the angular alignment.

SWGDS — Surface Wave Propagation Constants

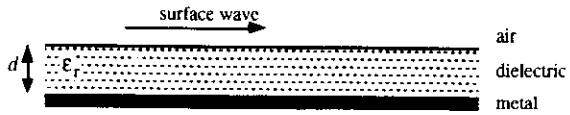

Figure 4.3 Dielectric slab on top of a ground plane

When a dielectric slab is placed on top of a ground plane, surface waves can propagate over and within the structure, and knowledge of their propagation characteristics is important in the design of surface wave antennas and printed antennas. When the signal frequency, the dielectric thickness and its permittivity are specified, the program determines the number of propagating surface wave modes and their propagating constants.

WIRE ANTENNAS

DIPOLE — Thin-Wire Dipole Characteristics

The input impedance is determined for a thin wire dipole of specified length and radius at a specified frequency. A Galerkin moment method is used for the analysis, and the uses specifies the number of piecewise sinusoidal (PWS) modes to be used. The dipole may be loaded with lumped loads at mode terminals and the feed point may be placed at any mode terminal. The program provides the mode currents, the radiation efficiency and the gain at broadside.

FLDDIPOL E[1] — Input Impedance of a Folded Dipole

A folded dipole is made of a dipole connected to a second wire conductor, making a rectangular loop (fig. 4.4).

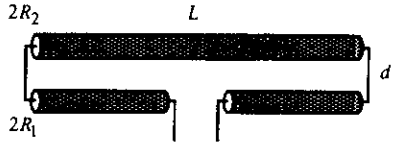

Figure 4.4 Folded Dipole

The program uses the same resolution technique as the previous one to determine the input impedance of the folded dipole, as a function of frequency, dipole length, radii of the two conductors and conductor spacing. The feed point is at the center of the dipole and there is no provision for lumped loading.

YAGI — Yagi-Udda Design

Yagi-Udda arrays are well known from their use with television receivers. They are formed of a dipole fed by a signal source and an array of rods (Fig. 4.5). A slightly longer rod placed on one side of the driven dipole acts as a reflector, while a series of shorter rods on the other side perform the task of directors.

The program calculates the gain, the back-to-front ratio and the input impedance of a Yagi-Udda array. The lengths and the spacings of the reflector, feed element, and directors are specified arbitrarily by the user. It is however assumed that all the direc-

[1] Some operating systems do not accept names with more than 8 letters, in which case the full name must be truncated.

tors have the same length and spacing. A method of moments procedure is used for the calculations.

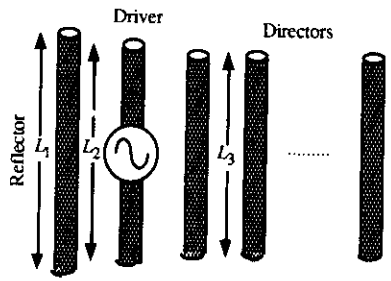

Figure 4.5 Yagi-Udda Antenna

LPDA — Log-Periodic Dipole Array Design

A log-periodic array of dipoles (fig. 4.6) provides antenna operation over a broad frequency bandwidth. All the elements of the array are connected to the signal source.

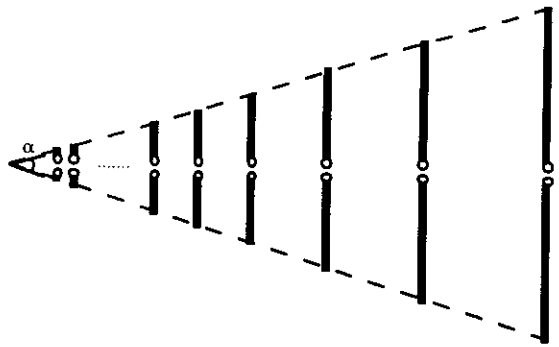

Figure 4.6 Log-periodic array of dipoles

The design of a log-periodic array must meet a specified gain over a frequency range, specified by its lower and upper frequencies. The program determines the required number of dipoles, their lengths, spacings and radii. The mutual coupling between radiating elements is not taken into account.

ARRAYS

ARRAY — Pattern of a Uniform Array

A set of N identical and equally spaced isotropic elements is considered, with uniform amplitude and linear phase taper. The scan angle and the beamwidth of the main beam are calculated and printed, while the radiation pattern is drawn. Even though this is the simplest possible design for an array, it has considerable practical and tutorial significance, as it can be used to visualize the effect of element spacing and phasing on beamwidth, beam pointing and side'obe levels.

NARRAY — Pattern of a NON-Uniform Array

This program similarly provides the pattern, scan angle and beamwidth of an array, but this time every element of the array can be arbitrarily situated and fed an arbitrary current. Inputs to the program are the frequency, the number of elements and, for each element, location, real and imaginary parts of the current. This is a very versatile program, but the user must enter a large amount of data.

CHEBY —Chebyshev Array Element Weights

Chebyshev synthesis yields the best possible compromise between sidelobe level and beamwidth by setting all the sidelobes at the same level. The elements are equally spaced, but fed currents having different amplitudes (weights). The user is requested to specify the number of elements, the spacing between elements in wavelengths and the sidelobe level in dBs. The element weights are calculated for all the elements and the resulting maximum directivity and the 3-dB beamwidth are determined. The array pattern obtained can also be plotted.

TAYLOR — Taylor-*N*-Array Element Weights

This program synthesizes a reduced sidelobe array using the Taylor-N technique. The approach is somewhat similar to the Chebyshev synthesis, but the relationship between beamwidth and sidelobe level is not optimal (but close to it), and it decreases away from breoadside. This results in a current distribution that may be easier to realize than the one for a Chebyshev array. The user is requested to specify the number of elements, the spacing between elements in wavelengths, the sidelobe level in dBs, and the desired value for the N coefficient. The weights are calculated for all the elements and the resulting maximum directivity and 3-dB bandwidth are determined. The array pattern obtained can also be plotted.

WOODLAW— Woodward-Lawson Array Pattern Synthesis

This method determines the relative current amplitudes that must be fed to the elements of an array to obtain a specified pattern, for instance a constant field pattern over a specified range, and zero elsewhere. The desired radiation pattern can be specified in either piecewise form or in sampled form. The element coefficients are printed out and the radiation pattern can be plotted to determine how well the requirement is met.

APERTURE ANTENNAS

APERTURE — Characteristics of Linear, Rectangular, and Circular Apertures

The half-power beamwidth, the sidelobe level and the directivity are calculated in terms of frequency and dimensions for linear, rectangular and circular apertures with uniform, triangular, cosine or cosine squared field distributions in the aperture.

HORN — Analysis and Design of Sectoral and Pyramidal Horns

At microwave frequencies the systems are often connected by waveguides (p'umbing), and then the easiest way to provide radiation is to flare the end of the waveguide to realize a horn. One can either change one dimension only — the width or the height — in which case one obtains a sectoral horn, or change both transverse dimensions to make a pyramidal horn (Fig. 4.7).

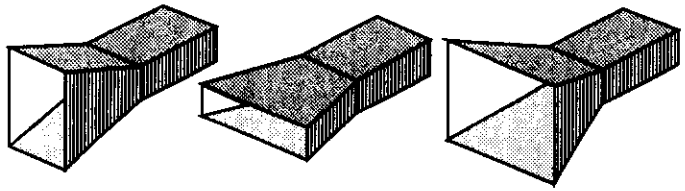

Figure 4.7 E-plane, H-plane sectoral horns and pyramidal horn

The antenna directivity is calculated and the E- and H-plane patterns are plotted for E- or H-plane sectoral horns and for pyramidal horns .The program uses rigorous expressions in terms of Fresnel integrals for the directivity and the far fields. The maximum phase error at the aperture edges and the optimum aperture size for maximum gain are also determined, The program cam also design a pyramidal horn corresponding to a desired gain and waveguide size, while corrugated horns can also be considered.

REFLECTO R[1] — Design of Prime-Focus Paraboloid Antenna

The performances of a prime-focus fed paraboloid antenna are determined in terms of frequency, dish diameter, *F/D* ratio (focal distance/dish diameter) and the characteristics of the feed. The program computes the spillover efficiency, the taper efficiency, the aperture efficiency and the directivity.

MSANT — Design of Rectangular Microstrip Antenna

Microstrip antennas (printed patch antennas) have become very popular due to their versatility, ruggedness and ease of fabrication. The program uses a version of the cavity model, valid for patch antennas on thin substrates, to determine the resonant frequency, the radiation resistance, the input impedance at the feed, the frequency bandwidth and the radiation pattern of a rectangular patch antenna. The user must specify the length and width of the patch, the dielectric constant and the thickness of the substrate, its loss tangent and the distance from feed to edge.

Remarks

The programs listed above were written in BASIC A, but can also run with other versions of BASIC. In all programs, the user is asked to answer a sequence of questions, to fully characterize the antenna to be analyzed or designed.

More information on microstrip patch antennas can be found in [2, 3], and a powerful computer program based on integral equation technique for the analysis of antennas printed on thick patches is now available [4].

References

[1] Pozar, D., Antenna Design using Personal Computers. Norwood, MA: Artech House 1985.

[2] James, J. R., and Hall, P. S., *Handbook of Microstrip Antennas*, London: Peter Peregrinus, 1989.

[3] Zürcher, J..F., and Gardiol, F., *Broadband Patch Antennas*. Norwood, MA: Artech House 1995.

[4] Jankovic, G., Wu, D. I., and Chang, D. C., "Computer-Aided Design of Probe-Fed and Loaded Microstrip Antennas in Multilayer Configurations", "*Proc. ANTEM'94*, Ottawa, Canada, August 1994, pp. 117–120.

---

[1] Some operating systems do not accept names with more than 8 letters, in which case the full name must be truncated.

LESSON 5: TUESDAY 7 FEBRUARY 1995

INTEGRAL EQUATION TECHNIQUES

The determination of the electromagnetic fields created by known currents in a homogeneous structure, i.e. formed of a single uniform medium of propagation, is directly provided by integral equations. Integral equation techniques can also be extended to analyze heterogeneous media, formed by the juxtaposition of several uniform media of propagation, by introducing equivalent sources. In the particular case of stratified media formed by a superposition of uniform layers, the stratified character of the structure can be taken into account in the integral formulation. The techniques developed are then applied to the analysis of printed circuits and antennas

Electromagnetic fields are generated by known impressed sources, represented by electric or magnetic surface currents. Since Maxwell's equations are linear, the resulting fields are expressed by superposition integrals of the known sources, weighted by Green's functions, which are space domain impulse responses.

1. HOMOGENEOUS MEDIUM

Maxwell's Equations and the Potentials

We consider a lossless homogeneous medium defined by a real permittivity ε and a real permeability μ. It is assumed that this medium does not contain either free charges or currents. Maxwell's equations are given in complex notation by:

$$\nabla\times\underline{\mathbf{E}} = -j\omega\mu\underline{\mathbf{H}} \qquad \nabla\cdot\underline{\mathbf{E}} = 0$$
$$\nabla\times\underline{\mathbf{H}} = j\omega\varepsilon\underline{\mathbf{E}} \qquad \nabla\cdot\underline{\mathbf{H}} = 0 \tag{5.1}$$

where the time-domain electric field of a signal of frequency $f = \omega/2\pi$ is expressed, in terms of the complex phasor-vector $\underline{\mathbf{E}}$

$$\mathbf{E}(\mathbf{r},t) = \mathrm{Re}\left[\sqrt{2}\,\underline{\mathbf{E}}(\mathbf{r})\exp(j\omega t)\right] \tag{5.2}$$

A **bold** character is a vector, while underlining indicates that a quantity is complex. The expression $\underline{\mathbf{E}}(\mathbf{r})$ is thus a complex vector, called a *phasor-vector*, and is a function of position $\mathbf{r}$. The spatial dependence of the field is entirely contained in $\underline{\mathbf{E}}(\mathbf{r})$. A phasor-vector can be developed either in terms of its three spatial complex components (for instance, in a rectangular system of coordinates) or in terms of its real and imaginary parts:

$$\underline{\mathbf{E}}(\mathbf{r}) = \mathbf{e}_x\underline{E}_x(\mathbf{r}) + \mathbf{e}_y\underline{E}_y(\mathbf{r}) + \mathbf{e}_z\underline{E}_z(\mathbf{r}) = \mathbf{E}_r(\mathbf{r}) + j\mathbf{E}_i(\mathbf{r}) \tag{5.3}$$

Maxwell's equations are partial derivative equations in three-dimensional space. The two curl ($\nabla\times$) expressions (left-hand side) specify relationships between spatial variations of a field (electric or magnetic) and the time-derivative ($j\omega$) of the other. The divergence ($\nabla\cdot$) expressions (right-hand side) indicate that there are no free charges.

The two Maxwell curl equations (on the left-hand side in Eqn. 5.1) are first-order partial derivative equations involving two different fields. One can combine them and obtain second-order equations in terms of either the electric or magnetic fields, which are called wave or Helmholtz equations:

$$\nabla\times\nabla\times\underline{\mathbf{E}} = -\nabla^2\underline{\mathbf{E}} = \omega^2\varepsilon\mu\underline{\mathbf{E}} \quad \text{and} \quad \nabla\times\nabla\times\underline{\mathbf{H}} = -\nabla^2\underline{\mathbf{H}} = \omega^2\varepsilon\mu\underline{\mathbf{H}} \tag{5.4}$$

Two potentials are often used to simplify further developments, namely the magnetic vector potential $\underline{\mathbf{A}}$ and the electric scalar potential $\underline{V}$, which are defined by:

$$\mu\underline{\mathbf{H}} = \nabla\times\underline{\mathbf{A}} \quad \text{and} \quad \underline{\mathbf{E}} + j\omega\mu\underline{\mathbf{A}} = -\nabla\underline{V} \tag{5.5}$$

The quantities $\underline{\mathbf{A}}$ and $\underline{V}$ are specified through differential operators: their definition is incomplete because one can add a constant term to $\underline{V}$ and, similarly, a curl-less (solenoidal) vector to $\underline{\mathbf{A}}$, without modifying the fields. Thus the potentials can be selected in a way that facilitates the resolution of the problem considered.

The potentials can be introduced within Maxwell's equations (5.1), which then yield two expressions containing both $\underline{\mathbf{A}}$ and $\underline{V}$. As one would generally prefer equations involving a single variable, the two expressions are combined and simplified through the introduction of a particular relationship called the *Lorentz Gauge* [5.1]:

$$\nabla\cdot\underline{\mathbf{A}} + j\omega\varepsilon\mu\underline{V} = 0 \tag{5.6}$$

Thus, the two following wave equations for the potentials are then obtained:

$$\nabla^2\underline{\mathbf{A}} + \omega^2\varepsilon\mu\underline{\mathbf{A}} = 0 \quad \text{and} \quad \nabla^2\underline{V} + \omega^2\varepsilon\mu\underline{V} = 0 \tag{5.7}$$

Spherical Waves in Free Space

Since waves are actually excited by localized sources, radiated fields are solutions of wave equation in spherical coordinates. The expression for the Laplace operator ∇^2 is then rather complex, but one obtains a simple expression when a purely

radial dependence is considered and the vectors are expressed by their rectangular components. The resulting magnetic vector potential and the electric scalar potential are given by:

$$\underline{\mathbf{A}}(\mathbf{r}) = \underline{\mathbf{A}}_0 \frac{\exp\left(-j\omega\sqrt{\varepsilon\mu}\, r\right)}{r} \quad \text{and} \quad \underline{V}(\mathbf{r}) = \underline{V}_0 \frac{\exp\left(-j\omega\sqrt{\varepsilon\mu}\, r\right)}{r} \tag{5.8}$$

To have a non zero solution one must have $\underline{\mathbf{A}}_0$ and $\underline{V}_0$ different from zero and the two potentials become singular at the origin of the coordinate system ($r = 0$), with first-order poles (in r^{-1}). This means that sources are located there: an infinitesimal electric current $\underline{\mathbf{J}}_\delta$, called Hertz dipole (source of the magnetic vector potential) and a point electric charge $\underline{q}$ (source of the electric scalar potential).

Carrying out the developments with source terms, Equation (5.8) yields:

$$\underline{\mathbf{A}}(\mathbf{r}) = \frac{\mu}{4\pi}\underline{\mathbf{J}}_\delta \frac{\exp\left(-j\omega\sqrt{\varepsilon\mu}\, r\right)}{r} \quad \text{and} \quad \underline{V}(\mathbf{r}) = \frac{\underline{q}}{4\pi\varepsilon} \frac{\exp\left(-j\omega\sqrt{\varepsilon\mu}\, r\right)}{r} \tag{5.9}$$

The vector potential $\underline{\mathbf{A}}(\mathbf{r})$ is parallel to the Hertz dipole at the origin of the coordinate system. This result is specific to the particular selection of vector potential that was made when introducing the Lorentz gauge.

When the sources are not located at the origin but at some point $\mathbf{r}'$, the resulting potentials are simply given by a linear translation. To do this, the radial coordinate r is simply replaced by the expression $|\mathbf{r} - \mathbf{r}'|$

$$\underline{\mathbf{A}}(\mathbf{r}) = \frac{\mu}{4\pi}\underline{\mathbf{J}}_\delta \frac{\exp\left(-j\omega\sqrt{\varepsilon\mu}\,|\mathbf{r}-\mathbf{r}'|\right)}{|\mathbf{r}-\mathbf{r}'|} \quad \text{and} \quad \underline{V}(\mathbf{r}) = \frac{\underline{q}}{4\pi\varepsilon} \frac{\exp\left(-j\omega\sqrt{\varepsilon\mu}\,|\mathbf{r}-\mathbf{r}'|\right)}{|\mathbf{r}-\mathbf{r}'|} \tag{5.10}$$

Then the electric and the magnetic fields are obtained by introducing the potentials obtained by using Equation (5.10) into Equations (5.5) and (5.3) and carrying out the calculations.

The electric and the magnetic fields also become singular at the location of sources, but since space derivatives are involved in their determination the poles are of second or third order. Calculations will be more difficult for the fields than for the potentials, even though the two approaches should eventually provide the same finite values. High-order poles introduce mathematical convergence problems that become particularly severe when expressions must be evaluated numerically.

Green's Functions

The magnetic vector potential produced at point $\mathbf{r}$ by a current density $\underline{\mathbf{J}}(\mathbf{r}')$ is expressed in integral form by:

$$\underline{\mathbf{A}}(\mathbf{r}) = \frac{\mu}{4\pi}\int_V \frac{\underline{\mathbf{J}}(\mathbf{r}')\exp\left(-j\omega\sqrt{\varepsilon\mu}\,|\mathbf{r}-\mathbf{r}'|\right)}{|\mathbf{r}-\mathbf{r}'|}\,dV' = \int_V \underline{\mathbf{J}}(\mathbf{r}')\underline{G}_{AJ}(\mathbf{r}-\mathbf{r}')\,dV' = \underline{\mathbf{J}} \otimes \underline{G}_{AJ} \tag{5.11}$$

This expression is a superposition integral in the space domain $\underline{\mathbf{J}} \otimes \underline{G}_{AJ}$, where the Green's function is the space-domain "impulse response". The primed coordinate $\mathbf{r}'$ specifies the location of the current density (sources) within the volume V', while the unprimed coordinate $\mathbf{r}$ is the position of the observer. The convolution of the Green's function $\underline{G}_{AJ}(\mathbf{r}-\mathbf{r}')$ with the current density $\underline{\mathbf{J}}(\mathbf{r}')$ yields the potential $\underline{\mathbf{A}}(\mathbf{r})$.

In free space, the Green's function for the vector potential is scalar, given by:

$$\underline{G}_{AJ}(\mathbf{r}-\mathbf{r}') = \frac{\mu}{4\pi}\frac{\exp\left(-j\omega\sqrt{\varepsilon\mu}\,|\mathbf{r}-\mathbf{r}'|\right)}{|\mathbf{r}-\mathbf{r}'|} \tag{5.12}$$

The exponential in the numerator takes care of the non zero propagation time, while the denominator represents the amplitude decay as the wave spreads out over a sphere of expanding area as it propagates away from the source point.

The corresponding magnetic field is obtain through derivation (5.5):

$$\underline{\mathbf{H}}(\mathbf{r}) = \frac{1}{\mu}\nabla \times \underline{\mathbf{A}}(\mathbf{r}) = \overline{\underline{\mathbf{G}}}_{HJ}(\mathbf{r}-\mathbf{r}') \otimes \underline{\mathbf{J}}(\mathbf{r}') \tag{5.13}$$

The Green's function $\overline{\underline{\mathbf{G}}}_{HJ}$ linking the magnetic field to the current is a tensor or *dyadic*, because the phasor-vectors $\underline{\mathbf{J}}$ and $\underline{\mathbf{H}}$ are not directed in the same direction. It is represented by a 3×3 matrix and is provided by:

$$\overline{\underline{\mathbf{G}}}_{HJ}(\mathbf{r}-\mathbf{r}') = \frac{1}{\mu}\nabla \times \left[\overline{\mathbf{U}}\,\underline{G}_{AJ}(\mathbf{r}-\mathbf{r}')\right] \tag{5.14}$$

where $\overline{\mathbf{U}}$ is the unit 3×3 dyadic and the differential operator ∇ operates only on the unprimed coordinates.

The electric field produced by an electric current density is obtained with (5.1):

$$\underline{\mathbf{E}}(\mathbf{r}) = \frac{1}{j\omega\varepsilon}\nabla \times \underline{\mathbf{H}}(\mathbf{r}) = \overline{\underline{\mathbf{G}}}_{EJ}(\mathbf{r}-\mathbf{r}') \otimes \underline{\mathbf{J}}(\mathbf{r}') \tag{5.15}$$

The electric field Green's function $\overline{\underline{G}}_{EJ}$, linking the electric field to the current, is also a tensor or *dyadic*. It is derived from the Green's function for the potential by:

$$\overline{\underline{G}}_{EJ}(\mathbf{r}-\mathbf{r}') = \frac{1}{j\omega\varepsilon\mu}\left(\nabla\nabla\cdot + \omega^2\varepsilon\mu\,\overline{\mathbf{U}}\right)\underline{G}_{AJ}(\mathbf{r}-\mathbf{r}') \tag{5.16}$$

Carrying out the derivations with respect to $\mathbf{r}$ yields a 3×3 matrix for the dyadic Green's functions. Some terms of the matrix have a third order pole at $\mathbf{r} = \mathbf{r}'$.

The electric scalar potential produced at point $\mathbf{r}$ by a charge density $\underline{\rho}(\mathbf{r}')$ is similarly expressed in integral form by:

$$\underline{V}(\mathbf{r}) = \frac{1}{4\pi\varepsilon}\int_{V'}\frac{\underline{\rho}(\mathbf{r}')\exp\left(-j\omega\sqrt{\varepsilon\mu}\,|\mathbf{r}-\mathbf{r}'|\right)}{|\mathbf{r}-\mathbf{r}'|}\,dV' = \int_{V'}\underline{\rho}(\mathbf{r}')\underline{G}_{Vq}(\mathbf{r}-\mathbf{r}')\,dV' = \underline{\rho}\otimes\underline{G}_{Vq} \tag{5.17}$$

The primed coordinate $\mathbf{r}'$ specifies the location of the charge density (sources) within the volume V', while the unprimed coordinate $\mathbf{r}$ is the position of the observer. The convolution of the Green's function $\underline{G}_{Vq}(\mathbf{r}-\mathbf{r}')$ with the charge density $\underline{\rho}(\mathbf{r}')$ yields the potential $\underline{V}(\mathbf{r})$. The Green's function for the scalar potential is given by:

$$\underline{G}_{Vq}(\mathbf{r}-\mathbf{r}') = \frac{1}{4\pi\varepsilon}\frac{\exp\left(-j\omega\sqrt{\varepsilon\mu}\,|\mathbf{r}-\mathbf{r}'|\right)}{|\mathbf{r}-\mathbf{r}'|} = \frac{1}{\varepsilon\mu}\underline{G}_{AJ}(\mathbf{r}-\mathbf{r}') \tag{5.18}$$

INHOMOGENEOUS STRUCTURES

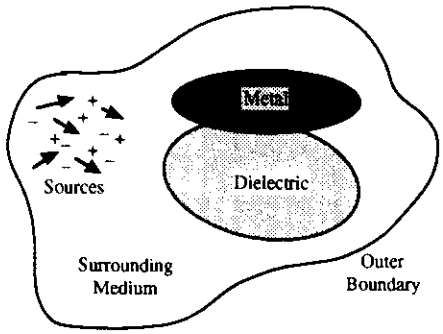

Figure 5.1 General inhomogeneous structure

Figure 5.1 shows a general heterogeneous structure. An inner domain contains a homogeneous dielectric, while another region is filled with conductor. The surrounding region is generally filled with air and is bounded by an outer enclosure, which can either be the sphere at infinity (open) or a metallic box.

Metallic Boundaries

The expressions derived until now provide the potentials and the fields produced by any combination of electric currents and charges located within a homogeneous medium. This means that when a distribution of currents and of charges is entirely specified (over all space) and when the surrounding medium is homogeneous, the potentials and, later on, the fields can be determined.

In many real-life problems, however, one considers metal surfaces (strips and patches) which are surrounded by inhomogeneous media. To satisfy the boundary conditions at the metal or at the dielectric interfaces, charges must be present and currents must flow on the conductors, but their distribution is not known beforehand.

On the surface of a good conductor, the tangential component of the electric field must satisfy a boundary condition, a suitable approximation of which is given by [5.2]:

$$\mathbf{n}\times\left(\underline{\mathbf{E}} - \underline{Z}_m\underline{\mathbf{J}}_s\right) = 0 \tag{5.19}$$

where $\underline{\mathbf{J}}_s$ is the surface current density, $\underline{Z}_m$ is the metal surface impedance, taking the finite conductivity of the metal into account, given by

$$\underline{Z}_m = \sqrt{j\omega\mu/\sigma} = (1+j)\sqrt{\omega\mu/2\sigma} \tag{5.20}$$

where μ is the permeability of the metal and σ is its effective conductivity, which must take into account the effect of surface roughness:

The boundary condition applies to the total electric field, which is the superposition of the field $\underline{\mathbf{E}}^{exc}$ produced by an excitation and the scattered or induced field $\underline{\mathbf{E}}^{scat}$ produced by currents and charges on the conductors.

Metallic surfaces can be handled in two quite different manners, depending on symmetry considerations.

The conductivity σ in most metals is so large and the electric field becomes vanishingly small inside the conductor (because the current density $\mathbf{J}$ must remain finite) that one sets $\sigma = \infty$ and then also $\mathbf{E} = 0$ within the conductor: this is a *perfect electric conductor* (PEC).

On the surface of a PEC, the tangential component of the electric field must be continuous. Since there is no field inside, the tangential component must also vanish outside, and the surface impedance Z_m in Equation (5.20) is equal to zero. Thus the electric field $\mathbf{E}$ is normal to the PEC boundary. The surface of a PEC generally supports an electric surface current $\mathbf{J}_s$.

The dual of the PEC is the *perfect magnetic conductor* (PMC), characterized by a vanishingly small internal magnetic field $\mathbf{H} \equiv 0$, in ferromagnetic materials for which the permeability μ is extremely large. In this case, the magnetic induction $\mathbf{B}$ must remain finite. When no current flows on the surface of a PMC, the tangential component of the magnetic field is continuous and must vanish. The magnetic field $\mathbf{H}$ is normal to the PMC boundary. In addition, the concept of the PMC remains useful to consider open circuit conditions.

Some structures possess a very large metallic ground plane, that extends under the complete circuit, and one can theoretically assume that it extends to infinity in the transverse directions. In addition, a ground plane made of perfect electric conductor (PEC, Z_m=0) behaves like a perfect mirror for the fields, and one can replace it by equivalent image sources (Fig. 5.2).

The two structures have the same fields above the ground plane and one can therefore replace the original structure by the equivalent structure with image sources. The Green's functions for the potentials and for the fields are therefore modified by adding the contribution of the images, provided by a vertical translation $2h$ and changes of sign to account for the polarity and the direction of the components.

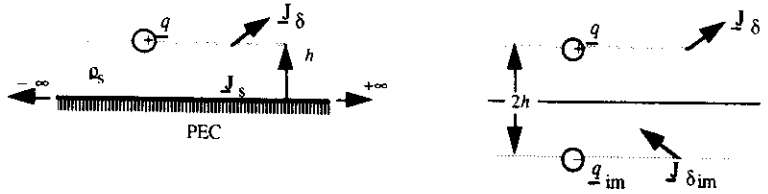

Figure 5.2 Equivalent images with an infinite ground plane.

The boundary condition on an infinite ground plane is thus included in the modified Green's functions, and there is no need then to determine the surface current. This reduces the number of equations to be solved, at the cost of a slight increase in the complexity of the Green's functions. When a modified Green's function satisfying a boundary condition is used in a superposition integral, any field obtained with this integral also satisfies the boundary condition.

Effects produced by edges of a real ground plane, which reflect and diffract the waves, cannot be taken into account, because the infinite ground plane considered has no edges. Other approaches are required to account for them.

When metallic boundary conditions cannot be included in the Green's functions, the metallic surfaces can be replaced by sheets of surface currents and charges. Adequate distributions of surface currents and charges must be selected so that the resulting total fields meet the conditions on the conductor boundaries.

Dielectric Media

The analyses of electromagnetic wave propagation considered an unbounded homogeneous medium in which the distributions of the fields were obtained by solving the wave equation for a homogeneous medium. This led to the definition of homogeneous Green's functions.

We consider now a structure made with several media, which are individually homogeneous but whose combination forms an inhomogeneous structure (Fig. 5.1). One must individually solve Maxwell's equations (or the wave equations) within each medium and then satisfy the boundary conditions, that require continuity of the tangential field components at the interfaces. This leads to a highly complex problem that can only be solved with advanced computer techniques. It is hardly worth mentioning that the homogeneous Green's functions previously defined are not valid in an inhomogeneous structure.

Two approaches extend the range of the previously described techniques to cover inhomogeneous structures.

- The first approach introduces "induced sources", replacing dielectrics by volume or surface polarization currents. The medium is then everywhere an homogeneous free space, in which the previously defined Green's functions can be used, but the polarization currents are new unknowns that must be determined.
- The second approach, valid in stratified media only, defines a modified Green's function in which the effects of the dielectric interfaces and ground plane are included.

A dielectric layer can be viewed as a distribution of polarization sources in free space (volume equivalence principle). Within the substrate, one replaces the dielectric by air, introducing at the same time an equivalent volume polarization current $\underline{\mathbf{J}}$ given by [5.3]:

$$\underline{\mathbf{J}} = j\omega\varepsilon_0(\varepsilon_r - 1)\underline{\mathbf{E}} \tag{5.21}$$

where $\underline{\mathbf{E}}$ is the total electric field existing in the dielectric, of relative permittivity ε_r. In this manner one obtains a homogeneous free space in which the Green's functions defined in Section 5.2 can be used. Then the unknown polarization current must be numerically determined, together with the unknown conduction surface currents on the metallic surfaces [5.4].

Huygens principle offers an alternative to the volume formulation for dielectrics in which one replaces the dielectric layers by magnetic and electric equivalent surface currents [5.5]. As in the previous section, one replaces, within the substrate, the dielectric by air; but on the air-dielectric interface one introduces equivalent surface electric and magnetic currents $\underline{\mathbf{J}}_{sd}$, $\underline{\mathbf{M}}_{sd}$ as follows:

$$\underline{\mathbf{J}}_{sd} = \mathbf{n} \times \underline{\mathbf{H}} \quad \text{and} \quad \underline{\mathbf{M}}_{sd} = -\mathbf{n} \times \underline{\mathbf{E}} \tag{5.22}$$

These currents radiate into an homogeneous medium, air, creating scattered fields that, when added to the excitation fields, reproduce the original total fields in the air and give null fields in the substrate.

Replacing a dielectric by polarization currents provides the only rigorous way to deal with edge effects due to finite dimensions of substrate and ground planes. The same approach can also analyze arbitrary distributions of permittivity and thick conductors. However, the use of equivalent polarization currents and free-space Green's functions yields problems of great numerical complexity that involve very large linear systems of equations [5.6]: although, since the available computer power increases at a tremendous rate, this drawback may no longer be too significant for small-sized problems.

Stratified Media Green's Function

At the beginning of the twentieth century, the German physicist Arnold Sommerfeld [5.7] formulated rigorous expressions for fields produced by a wire above a transversely infinite lossy ground, based on the concept of the Sommerfeld identity

Extending his approach, the boundary conditions for stratified dielectric layers (Fig. 5.3) and the ground plane can be included in the Green's functions, yielding Sommerfeld integrals or Hankel transforms [5.8]. This approach implicitly assumes that the dielectric slab and the ground plane must both extend to infinity along the transverse directions

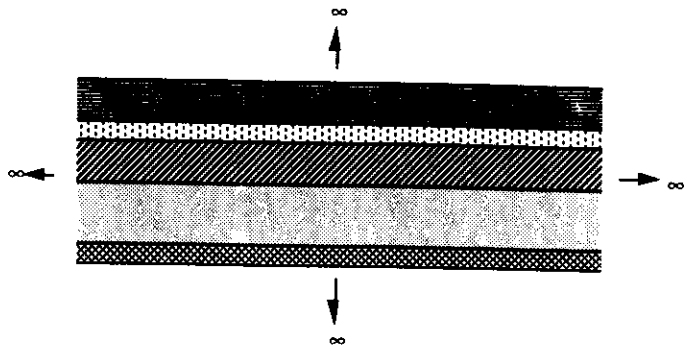

Figure 5.3 Stratified Media

A Sommerfeld integral $\underline{S}_n(\underline{F})$ takes the general form:

$$\underline{S}_n(\underline{F}) = \int_C \mathrm{H}_n^{(2)}(\underline{\xi}\rho)\,\underline{\xi}^{n+1}\,\underline{F}(\underline{\xi})\exp\left(-\sqrt{\underline{\xi}^2-\omega^2\varepsilon\mu}\,|z|\right)\mathrm{d}\underline{\xi} \tag{5.23}$$

where C is a carefully selected integration contour in the complex plane of the integration variable $\underline{\xi}$. For instance, the Sommerfeld identity (Eqn. 5.13) is the Sommerfeld integral $\underline{S}_0[(\underline{\xi}^2-\omega^2\varepsilon\mu)^{-1/2}]$ integrated over the infinite real axis. The functions to be integrated generally possess singularities and sometimes also exhibit a diverging behavior for increasing values of the argument (Fig. 5.4).

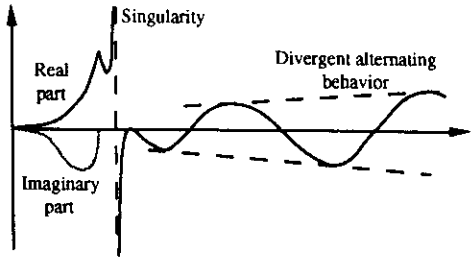

Figure 5.4 Example of integrand in Sommerfeld integral.

The functions to cannot be integrated analytically and their diverging behavior precludes the direct use of a numerical integration scheme. Their badly behaved dependence led to the development of spectral domain approaches [5.9], in which the trans-

verse coordinate description of the structure is transformed by a two-dimensional Fourier transform. Asymptotic expansions were also developed to determine the far-field distribution [5.10].

The first attempts to evaluate numerically Sommerfeld integrals in the space domain were carried out by Mosig [5.11], who introduced bending-around-the-pole and averaging techniques to take care of the singularity and of the diverging behavior at infinity. This approach led to efficient and accurate computer algorithms. Similar techniques to evaluate Sommerfeld integrals were developed by other authors [5.12].

Many other approaches have recently become available to accurately compute Sommerfeld integrals [5.13, 5.14], and closed form asymptotic approximations have been developed [5.15]. The complex image method, based on exponential approximations with Prony's method or with pencil of functions [5.16] provides an acceleration by a factor of 10–15 times with respect to numerical integration but requires some "fine tuning" [5.17].

Statement of the Problem

One must still determine which distribution of the currents flowing on the conductors produces a total field that satisfies all the boundary conditions. To do this, the Green's function equations are introduced into the boundary equations, using either homogeneous or inhomogeneous, either for the electric field or for the potentials.

In the *electric field integral equation* formulation (EFIE) the electric field produced by the surface currents is replaced by its expression eqn. (5.19) to yield :

$$\mathbf{n}\times\left(\underline{\mathbf{E}}^{\text{exc}}+\underline{\mathbf{E}}^{\text{scat}}-\underline{Z}_{\text{m}}\underline{\mathbf{J}}_{\text{s}}\right)=\mathbf{n}\times\left(\underline{\mathbf{E}}^{\text{exc}}+\overline{\overline{\mathbf{G}}}_{EJ}\otimes\underline{\mathbf{J}}_{\text{s}}-\underline{Z}_{\text{m}}\underline{\mathbf{J}}_{\text{s}}\right)=0 \tag{5.24}$$

The field at the surface of the conductors is determined by the current flowing within the very same conductors: one must in particular determine the effect of a point upon itself — in which case the distance from source to observer vanishes. Some components of the dyadic Green's function $\overline{\overline{\mathbf{G}}}_{EJ}$ show singularities of the $|\mathbf{r}-\mathbf{r}'|^{-3}$ type, which precludes a direct evaluation in the space domain of the superposition integral [5.18].

The effect of strong singularities for the electric field can be circumvented with the *spectral-domain approach*. The whole plane of the interface (assumed to be infinite in the two transverse directions) is considered and a two-dimensional Fourier transform is applied to the boundary condition [5.19].

The currents on the upper conductor are also expressed by a Fourier transform, and all subsequent developments are carried out in the transformed spectral domain. This method was used to analyze antennas [5.20] and is particularly useful with geometries where the Fourier transform can be defined.

Another manner to avoid strong singularities is to use the magnetic vector potential $\underline{\mathbf{A}}$ and of the electric scalar potential $\underline{V}$ in the *mixed potential integral equation* formulation (MPIE). The boundary value equation then yields, after some developments:

$$\mathbf{n}\times\left[\underline{\mathbf{E}}^{\text{exc}}+\text{j}\omega\overline{\overline{\mathbf{G}}}_{A}\otimes\underline{\mathbf{J}}_{\text{s}}+\nabla\left(\underline{G}_{V}\otimes\underline{q}_{\text{s}}\right)-\underline{Z}_{\text{m}}\underline{\mathbf{J}}_{\text{s}}\right]=0 \tag{5.25}$$

where the surface charge density $\underline{q}_{\text{s}}$ is associated to the surface current through the continuity equation. This formulation is a logical extension of the MPIE introduced by Harrington [5.21] for wire antennas in free space. Calculations in the space domain are always possible if the potentials $\underline{\mathbf{A}}$ and $\underline{V}$ are introduced because then Green's functions only exhibit mild singularities of the $|\mathbf{r}-\mathbf{r}'|^{-1}$ type, which can easily be eliminated when computing the superposition integrals.

Green's functions for the potentials exhibit azimuthal symmetry, depending on the x, y coordinates only through the radial distance $\rho=\sqrt{x^2+y^2}$. Therefore, they can be computed and stored in one-dimensional tables when analyzing a single-layer structure.

The surface current $\underline{\mathbf{J}}_{\text{s}}$, that one wishes to determine, appears within superposition integrals, which cannot be simply inverted extract $\underline{\mathbf{J}}_{\text{s}}$, and more involved developments are required. In the method of moments (MoM) [5.21], the unknown current is expanded over a set of basis functions, and the same is done for the unknown surface charge density:

$$\underline{\mathbf{J}}_{\text{s}}=\sum_{i=1}^{M}\underline{\alpha}_i\,\underline{\mathbf{J}}_{si}\qquad \underline{q}_{\text{s}}=\sum_{i=1}^{M}\underline{\alpha}_i\,\underline{q}_{si} \tag{5.26}$$

The basis functions $\underline{\mathbf{J}}_{si}$ form part of a complete set, and the charge densities $\underline{q}_{si}$ are related through the continuity equation. The unknown coefficients $\underline{\alpha}_i$ have to be determined from the boundary conditions. For obvious practical reasons the series must be truncated and the number of terms M necessary to achieve the desired accuracy determined through successive computations.

For conductors having a simple geometry trial functions may be defined over the whole surface and are then called *entire domain basis functions*. For instance, the

current on a rectangular patch is expressed by a two-dimensional Fourier series, while series of Hankel functions are used with cylindrical or annular patches.

Irregular geometries, on the other hand, are divided into rectangular or triangular subsections. Within each subsection, the current either varies linearly as a function of position or is expressed by a more involved polynomial expansion. Overlapping rooftops covering two adjacent cells are often used to develop the surface currents in perpendicular directions, yielding pulse doublets for the associated surface charge density (Fig. 5.5).

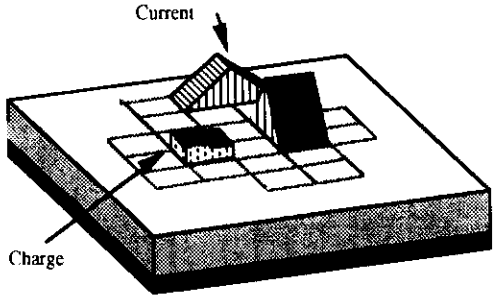

Figure 5.5 Definition of rectangular subsectional basis functions.

Elementary cells can be all rectangular with the same size, rectangular with different sizes [5.22], or still take a triangular shape. The actual selection results from a compromise between computation complexity and ability to represent accurately the actual conductor shape. Combinations of different cell shapes and of subdomain and entire domain basis functions have also been considered.

The boundary condition cannot be exactly satisfied at every point on the conductor, so in practice one multiplies it by a "test function" and integrates it over the domain of this test function. In this manner, one satisfies the boundary condition in a "weak sense" because only a weighted average value is controlled. The test function set may be identical to the basis function set, thus leading to a Galerkin procedure. Another common choice, when subsectional basis functions are used, is to integrate the boundary condition along segments joining the centers of adjoining subdomains (razor test procedure). In all cases, one obtains a set of M linear equations for the M unknowns, which is symbolically written in the following matrix form:

$$[\underline{Z}^{\mathrm{MoM}}][\underline{\alpha}] = [\underline{V}] \tag{5.27}$$

where the vector $[\underline{V}]$ represents the excitation. This matrix equation is solved to yield the current and charge distributions on the microstrip patch or strip. Then the quantities of interest to characterize circuits (impedance or scattering matrix) and those for antennas (gain, radiation pattern) are determined from the current distribution.

Numerical Aspects

Most techniques used to analyze antennas and circuits require the resolution of systems of linear equations. If the number of unknowns is not too large, this is done by matrix inversion. Standard software packages provide algorithms to do this.

When the number of unknowns becomes very large, matrix inversion requires an extremely large memory space and becomes either impractical or extremely time consuming. However, the matrices have a block structure including null submatrices and regions where numbers are negligibly small, so iterative techniques like overrelaxation or biconjugate gradient methods can be successfully implemented.

Moreover, some discretization schemes yield symmetric matrices that have Toeplitz properties, while reciprocity properties of the electromagnetic fields introduce redundancies in the matrix elements. One may take advantage of these properties to reduce the size of the system and, thus, the memory size and the computation time.

The resolution of the matrix equations, even with accelerating techniques, takes considerable more computing time than the evaluation of Sommerfeld integrals. As a result, the gain in time provided by fast evaluation techniques like the complex image method is not significant when compared to the total computer time required [5.17].

Integral equation techniques produce results with errors well within manufacturer's tolerances for the substrates, and since full wave solutions are complete, they model all physical parameters that affect the antenna performance. This high accuracy and reliability comes at the expense of increased computer processing time. However, as more powerful computers become readily available, the suitability of full wave analysis for microstrip antennas and circuits is obvious.

Input Impedance

The computations described in the previous sections yield the surface current density on the microstrip upper conductor (strips and patches) resulting from a specified excitation, most often a unit current (1 A) injected by the feed system. The voltage appearing across the conductors of the input port is then the input impedance, which is determined by integrating the electric field obtained by the method of moments [5.22].

Theoretical developments traditionally considered coaxial feeds, often modeled by a vertical filament of unit current terminated by a point charge acting on some point of the upper conductor. This simple model does not take into account the self term of the input impedance because the charge distribution is singular. Therefore, one can introduce an attachment mode between the coaxial pin and the upper conductor, which becomes an additional unknown in the procedure, thus increasing its complexity [5.23].

Undue complexity can be avoided by modeling the coaxial probe by a vertical current filament of unit density acting on the center of an elementary cell and spreading the associated point charge with a constant density over the entire cell. The continuity equation is satisfied globally over the complete cell but is not satisfied locally. The input impedance is obtained by integrating the electric field tangent to the vertical filament between the ground plane and the upper conductor, which leads to a quadratic form for the computation of the impedance.

More recently, line feeds were also considered in some detail and several approaches for its analysis were proposed. In the two-point impedance average, the potential is calculated at several points on the feed line and divided by the current distribution on the line. The line can also be terminated by a coaxial probe and deembedding used to find the impedance on the line. The three-point method compares three samples of the current distribution and approximates the amplitudes of the forward and reverse traveling waves on the line. It can be improved upon by using a singular value decomposition. Finally, Prony's method also determines the characteristics of higher order modes. A recent publication compares these approaches [5.24].

An antenna may have more than one connection to the feed network: for instance, in the cases of dual polarized antennas and antenna arrays (Chaps. 6 and 7). In this case, one sequentially feeds the different ports and determines the voltages appearing across each of them. This provides the impedance matrix, in terms of which one can determine the scattering matrix [5.25].

Far-Field Pattern

When the electric surface current on the microstrip upper conductor is known, the electric and the magnetic field can be determined everywhere in space, making use of the Green's function formulations. To determine the far-field radiation pattern of the antenna, however, calculations are considerably simplified by using asymptotic techniques, such as the steepest-descent method [5.26]. The application of this method to the Sommerfeld integrals used in the analysis of microstrip patch antennas is presented in some detail in [5.13].

CAD Software

A CAD tool, called "Ensemble", for the analysis of multilayer antennas with vertical probe was recently reported [5.27]. It consists of a graphical user interface and a full-wave simulator based on the integral equation formulation and moment method approach described here. The simulator is modular, accurate, versatile, efficient, and adaptable to different antenna substrate configurations. A simulation program has been developed to analyze two-layer microstrip structures with complex permittivity substrates and imperfect conductors that are fed by microstrip lines and coaxial probes. The program uses a mix of rectangular and triangular cells to discretize the structure, which allows the user to model irregularly shaped radiating elements and feed networks. A sophisticated attachment mode is used to satisfy the continuity of the current at the junction between the probe feed and the patch.

MININEC

Introduction

The Numerical Electromagnetics Code (NEC) [5.28] is probably the most advanced computer code available for the analysis of thin wire antennas. It is a computer code offering a comprehensive capability for the analysis of the interaction of electromagnetic waves with conducting structures. The program is based on a numerical solution of integral equations for the currents induced by an excitation field on a structure made of smooth surfaces and thin wires.

A NEC model may include nonradiating networks and transmission lines, perfect and lossy conductors, lumped elements and ground planes, which may either be perfect or lossy conductors. The excitation may be an applied voltage or an incident plane wave. The program determines the induced currents and charges, and then the near or far zone electric and magnetic fields. Other antenna parameters like the gain and directivity, power efficiency and coupling can then also be determined.

In many problems, however, the extensive capability of NEC is not required, either because the structure considered is not very complex, or because a simplified model is sufficient to obtain the information required. In addition, NEC requires access to a large main-frame computer and a FORTRAN compiler.

The MININEC system offers many of the NEC options, but makes use of a BASIC language that is compatible with most popular microcomputers. It is suitable for "small" problems on small computers compatible with the IBM PC format. The Naval

Ocean Systems Center (NOSC) has made the code available to the public [5.29]. The MININEC system is also distributed commercially by Artech House [5.30] and version 3.13 and GRAPS 2.0 is included in the CAEME Software Book [5.31]. Added features were provided by the Applied Computational Electromagnetics Society (ACES).

Overview

MININEC is a method of Moments code for the analysis of thin wire antennas using a Galerkin procedure suggested by Wilton [5.32]. The Electric Field thin wire integral equation is solved for the wire currents. Because it is written in BASIC, it is limited to less than 75 unknowns and 10 wires, depending on the computer memory size and the BASIC compiler (larger problems can be solved with NEC, which however is not as user-friendly and might tend to intimidate a beginner).

Since electromagnetics can best be understood with graphical means, the package GRAPS [5.33] is included in CAEME as an adjunct to MININEC. Plotters supporting the HPGL command set and printers with Epsom-compatible dot matrix capability can be used as output devices for GRAPS. The executable version of the codes requires a math co-processor.

Method of Resolution

MININEC uses a numerical solution method of an integral equation of electric fields presented by Harrington [5.21]. The following assumptions are made:

- The wire radius is very small with respect to the wavelength ($\leq 0.001\ \lambda$) and with respect to the wire length,
- The wire is subdivided into short segments, and the wire radius must also remain small with respect to the length of any segment. One can then assume that the currents are directed along the wires and that there are no circumferential currents flowing around the wires.

The electric field is obtained from the scalar electric potential and the magnetic vector potential, calculated by potential equations derived from the Helmholtz wave equations for known current and charge distributions. The electric field on a wire is produced by three sources: (1) current and charges on the wire and on nearby wires, (2) incoming waves from distant or nearby radiators, and (3) local sources of electric fields on the wire.

The currents on the wires are not known beforehand, but are actually the unknowns that must be determined in the problem. This is done by imposing the boundary condition on the conductors, i.e. by letting the tangential electric field components vanish on the perfect electric conductor (pec) surfaces. For thin wires, the total axial electric field, resulting from the three sources mentioned previously, must equal zero on the wire surfaces. This provides an integral representation for the currents and charges, which is solved by the method of moments (MOM), also known in linear algebra as the method of equality of projections.

The MOM solution in MININEC replaces the unknown currents by complex constants or "current pulses" centered on the ends of the segments. The charges are also complex constants (pulses), centered on the middle of the segments. The integrals are solved by numerical integration for the complex matrix constants that describe the unknown currents, yielding mutual and self interaction terms: electric field on one segment produced by the current on an other segment and by the current on the same segment. These terms form an "impedance matrix", and the currents are then obtained by matrix inversion.

Ground planes are taken care of by the method of images. Lumped impedances can be added at junctions between connecting segments.

When the currents and charges on the wires are known, the electric and the magnetic fields can be determined, both in the near and in the far zones. The quantities of interest in antenna design can then also be obtained.

Modeling and Limitations

Methods of moments are approximations: the currents are discretized as a set of pulses, that are only an approximate representation of the actual currents. The following items determine how closely the computer solution can represent the actual performance:

- The numerical methods employed and how well these methods are implemented on the computer,
- The inherent accuracy of the computer (rounding errors),
- How well the antenna being modeled conforms to the simplifying assumptions of the electromagnetic formulation of the program.
- The user's experience in recognizing problem areas (for instance, the wire sections should be shorter in locations where the current is expected to have strong variations, and may be longer elsewhere).

The user should always remain fully aware of potential difficulties in the modeling process, from initial setup to output interpretations. A new user should gain experience by running MININEC for a number of problems and comparing the results obtained with other computer solutions or with experimental data. When some confidence has been gained through experience, new problems can be tackled, but always with care and caution.

Some practical advice:

- Use between 10 and 20 segments on a halfwave dipole for accurate input impedance and power gain.
- Antiresonant dipole solutions (full-wave) will not converge.
- The wire radius must not exceed l/1000, otherwise the thin-wire criteria are violated.
- The segment length should be at least 10 times the radius.
- The segments should not be shorter than 10^{-4} wavelengths.
- Results given by MININEC may not be accurate when the spacing between parallel segments is less than l/10.
- Collinear connecting segments of different radii (tapered wires) seem to be accurately modeled as long as requirement 3 is satisfied.
- Loop antennas approximated by polygons show accurate input impedance from 7 wavelengths down to 0.01 wavelengths.
- Near field calculations for a short vertical whip antenna agree within 10% of measured fields for distances as close as 0.01 wavelength. When the observation distance is at one radius from the wire surface, MININEC's near-field calculations fail and must not be used.

A well known antenna manufacturer indicates that in the design of Yagi antennas, MININEC results for gain and pattern were found to be within 1 dB of the measured values. The input impedance is not predicted as accurately, because feed systems are generally too complex to be accurately modeled with MININEC.

Example of Application : Thin Wire Half Wave Dipole

1. Start MININEC by selecting option C in the main CAEME menu. Set the CAPS LOCK key on (MININEC only responds to instructions in capital letters). Answer the questions as they are presented.
2. To the question DO YOU WANT TO CREATE A GEOMETRY FILE? answer by typing N. Output should go to the console, C. MININEC asks for the frequency in MHz; The default value is 299.8 (1 metre wavelength), obtained by the ENTER key. This is a convenient choice which allows the geometry of the wires to be put in wavelengths. Length units are always in metres in MININEC.
3. The ENVIRONMENT can be selected as FREE SPACE (1) or a ground plane, perfect or lossy (-1). select 1, FREE SPACE. The next question is DO YOU WISH TO LOAD A GEOMETRY FILE?, and the answer is Y. Name of the geometry is DIPOLE.INP (provided on the disk).
4. The screen scrolls off the wire coordinates, assuming the standard rectangular coordinates X, Y, Z. The dipole selected has 20 segments, 19 pulses (current sample points) and two open ends. Pulse 10 is the center pulse, which will be excited by a voltage generator. To the CHANGE GEOMETRY? question, type N. The number of sources is 1. The PULSE NO., VOLTAGE MAGNITUDE, PHASE? response is 10, 1, 0. Any value of voltage source will provide the current shape and the correct input impedance, and specific feed point values are of concern only for arrays with multiple feeds.
5. The NUMBER OF LOADS response is 0, and we want the current computed, C. The matrix is then filled and factored with MININEC providing the timing data. For this small problem the time is quite short, but when larger geometries are considered, the computing time becomes substantial. VOLTAGE, CURRENT, IMPEDANCE and POWER are displayed. If you want to save the impedance data for later convergence tests, you could choose (but not now) Y and a file name (suc as DIPOLEZ). The question NEW OR OLD FILE will either start the file (N), if this was the first case, or (O) add impedance data to an ongoing study. Here we choose N for the answer to the SAVE IMPEDANCE TO A FILE? question.
6. The current values are then listed, starting from zero at the open ends of the dipole and taking its maximum value at the pulse 10, at the center feed point. The phase distribution is fairly uniform, as would be expected for a standing wave pattern. It is not necessary to save the currents at this point, so choose N.

7. Let us create a horizontal (azimuth plane) far field pattern for the dipole by choosing P from the MININEC MENU. We take the pattern in dBi (dBs with respect to an isotropic radiator) and type D. The ZENITH ANGLE? query refers to the theta angle in the spherical coordinate system. Our sample dipole lies along the Y axis, centered about the Z-X plane, and we select q = 90° by typing 90,0,1. The AZIMUTH ANGLE? is the f angle of the spherical coordinate system. To have a complete coverage without break, we must take it from 0° to 361°, which gives as instructions, with a step of 10: 0,10,37. For a smooth printout, 1° steps would be recommended. The FILE PATTERN question is answered N because our plot (DIPOLE.OUT) is already prepared for this demonstration. If you answer Y, you will be prompted for an output file and should then use DIPOLE.OUT. This file will now serve as input to the post processor which creates a data file for plotting.

8. The pattern values scroll by, showing -147 dBi for the endfire nulls and 2.15 dBi for the broadside maxima, as expected. (-147 dBi is not exactly zero, but is the smallest value that can be numerically obtained from MININEC on a PC). Let's quit, Q, and look at the current and far-field plots.

9. After Q, the post processor automatically runs (or type MNPOST at the DOS prompt) and requests MININEC output data file. The output file/s you used for MININEC should be used in this program for plotting. Follow the steps in the post processor to generate a name.DAT file for use in GRAPS. For this particular example, type Control C to get out of MNPOST.

10. Choose Option B from the submenu or type GRAPS from the DOS prompt for the plotting program and choose F1 to select the name you will plot. The name is DIPOLEP. Notice that the name of the file appears at the bottom right of the screen, and the GRAPH TYPE is automatically set to POLAR. Press F3 for a screen plot (if the circles come out as ellipses, the vertical or the horizontal size controls must be adjusted). The broadside direction is vertical and the endfire is horizontal. This particular plot was drawn with 361 points and is smooth. Then clear the screen by pressing F10 and then F1 to select a new file for plotting. Type DIPOLEC to retrieve the currents setup for the demonstration, and press F3 to display the plot on the screen. Pressing F10 will return to the GRAPS main menu. Press F10 again and ENTER to leave GRAPS.

References

[5.1] Stratton, J. A., *Electromagnetic Theory*, New York: McGraw Hill, 1941.

[5.2] Mosig, J. R., "Arbitrarily Shaped Microstrip Structures and their Analysis with a Mixed Potential Integral Equation", *IEEE Trans. on Microwave Theory and Techniques*, Vol. **36**, 1988, pp 314–323.

[5.3] Balanis, C. A., *Advanced Engineering in Electromagnetics*, New York: Wiley, 1989

[5.4] Kishk, A. A., and L. Shafai, "Different Formulations for Numerical Solution of Single or Multibodies of Revolution with Mixed Boundary Conditions", *IEEE Trans. on Antennas and Propagation*, Vol. **34**, 1986, pp. 666–673.

[5.5] Sarkar T. K., and E. Arvas, "An Integral Equation Approach to the Analysis of Finite Microstrip Antennas", *IEEE Trans. on Antennas and Propagation*, Vol. **38**, 1990, pp. 305–312.

[5.6] Mosig, J. R., "Integral Equation Techniques for Three-Dimensional Microstrip Structures," in R. Stone, Ed., *Review of Radio Science 1990–1992*, London: Oxford University Press, 1993, pp. 127–152.

[5.7] Sommerfeld, A., "The Propagation of Waves in Wireless Telegraphy", *Ann. Physik* (4), Vol. **28**, 1909, p. 665.

[5.8] Sneddon, I., *The Use of Integral Transforms*, New York: McGraw Hill, 1972.

[5.9] Itoh, T. "Spectral Domain Immitance Approach for Dispersion Characteristics of Generalized Printed Transmission Lines", *IEEE Trans. on Microwave Theory and Techniques*, Vol. **29**, 1980, pp. 496–499.

[5.10] Uzunoglu, N. K., N. G. Alexopoulos, and J. G. Fikioris, "Radiation Properties of Microstrip Dipoles", *IEEE Trans. on Antennas and Propagation*, Vol. **27**, 1979, pp. 853–858.

[5.11] Mosig, J. R., "Asymptotical Expansions for Rapidly Varying Integrands," *Abstracts of IEEE 1979 AP-S Internat. Symp.*, June 1979, pp. 177–180.

[5.12] Alexopoulos, N. G., and I. E. Rana, "On the Solution to Pocklington's Equation for Antennas Printed on Grounded Substrates," *Abstracts of IEEE 1979 AP-S Internat. Symp.*, June 1979, pp. 171–174.

[5.13] Mosig, J.R., R.C. Hall, and F.E. Gardiol, "Numerical Analysis of Microstrip Patch Antennas," in J. R. James and P. S. Hall, Eds., *Handbook of Microstrip Antennas*, London: Peter Peregrinus, 1989.

[5.14] Li, Y. C., C. H. Liu, and S. J. Franke, "Adaptive Evaluation of the Sommerfeld-Type Integral Using the Chirp-Z Transform", *IEEE Trans. on Antennas and Propagation*, Vol. **39**, 1991, pp. 1788–1792.

[5.15] Barkeshli, S. P., P. H. Pathak, and M. Marin, "An Asymptotic Closed-form Microstrip Surface Green's Function for the Efficient Moment Method Analysis of Mutual Coupling in Microstrip Antennas", *IEEE Trans. on Antennas and Propagation*, Vol. **38**, 1990, pp. 1374–1383.

[5.16] Chow , Y. L., J. J. Yang, D. G. Fang, and G. E. Howard, "A Closed-form Spatial Green's Function for the Thick Microstrip Substrate", *IEEE Trans. on Microwave Theory and Techniques*, Vol. **39**, 1991, pp. 588–592.

[5.17] Gay-Balmaz, P., Michalski, K., and J. R. Mosig, "On the Performance of the Discrete Complex Image Method in the Integral Equation Analysis of Microstrip Patch Antennas," *Abstracts of PIERS'94, Progress in Electromagnetics Research Symp.*, July 1994, p. 168.

[5.18] Van Deventer, T. E., P. B. Katehi, and A. C. Cangellaris, "An Integral Equation Method for the Evaluation of Conductor and Dielectric Losses in High-Frequency Interconnects", *IEEE Trans. on Microwave Theory and Techniques*, Vol. **37**, 1989, pp. 1964–1972.

[5.19] Uwano, T., and T. Itoh, "Spectral Domain Approach", in T. Itoh, Ed., *Numerical Techniques for Microwave and Millimeter Wave Passive Structures*, New York: Wiley, 1989.

[5.20] Araki, K., and T. Itoh, "Hankel Transform Domain Analysis of Open Circular Microstrip Radiating Structures", *IEEE Trans. on Antennas and Propagation*, Vol. **25**, 1981 pp. 84–89.

[5.21] Harrington, R. F., *Field Computation by Moment Methods*, New York: Macmillan, 1968.

[5.22] Skrivervik, A., and J. R. Mosig, "Impedance Matrix of Multiport Microstrip Discontinuities Including Radiation Effects", *Archiv für Elektronik und Ubertragungstechnik*, Vol. **44**, 1990, pp. 453–461.

[5.23] Hall, R. C. and J. R. Mosig, "Vertical Monopoles Embedded in a Dielectric Substrate", *IEE Proc.*, Vol. **136**, pt. H, 1989, pp. 462–468.

[5.24] Hall, R. C., and J. R. Mosig, "Impedance De-embedding Techniques in the Analysis of Microstrip fed Patch Antennas", *Abstracts of PIERS'94, Progress in Electromagnetics Research Symp.*, July 1994, p. 166.

[5.25] Gardiol, F. E., *Microstrip Circuits*, New York: Wiley, 1994.

[5.26] Felsen, L. B., and N. Marcuvitz, *Radiation Scattering of Waves*, Englewood Cliffs, NJ: Prentice Hall, 1973.

[5.27] Jankovic, G., D. I. Wu, and D. C. Chang, "Computer-Aided Design of Probe-Fed and Loaded Microstrip Antennas in Multilayer Configurations", "*Proc. ANTEM'94*, Ottawa, Canada, August 1994, pp. 117–120.

[5.28] Burke, G.J. and A.G. Poggio, "Numerical Electromagnetics Code (NEC)-Method of Moments", NOSC (Naval Ocean Systems Center) TD 116, January 1981.

[5.29] Rockway, J.W., J.C. Logan, "The new MININEC (Version 3): A Mini-Numerical Electromagnetics Code", NOSC (Naval Ocean Systems Center) TD 938, September 1986.

[5.30] Rockway, J.W., J.C. Logan, D.W.S. Tam and S.T. Li, *The MININEC System: Microcomputer Analysis of Wire Antennas*", Norwood, Artech House, 1988.

[5.31] Adler, R.W., "Mininec" in: Iskander, M., editor, *NSF/IEEE Center for Computer Applications in Electromagnetic Education, Software Book*, vol. I, ch. 14, 1992.

[5.32] Wilton, D. R. "Wire Problems", Lecture notes for short course on computational methods in Electromagnetics, 1981.

[5.33] Logan, J.C. and J. Strauch, "GRAPS User's Guide - A graphical plotting system for displaying scientific and engineering data", NOSC (Naval Ocean Systems Center) TD 1326,October 1988.

LESSON 6: WEDNESDAY 8 FEBRUARY 1995

ATMOSPHERIC PROPAGATION

The atmosphere is not homogeneous

Contrary to popular belief, the dielectric permittivitty of air is not identical to ε_0, nor is its refractive index exactly equal to 1. In many practical applications, this approximation is quite sufficient but, when considering long propagation paths in the atmosphere (tens of kilometers or more) the variation of the refractive index with altitude plays a significant role. The propagation paths are no longer straight, but become curved trajectories, lengthening the transmission range.

The refractive index of air n was determined experimentally, and is approximately given by the following expression, valid for radio waves:

$$n = 1 + \left(\frac{79p}{T} - \frac{11e}{T} + \frac{3.8\,10^5}{T^2} \right) 10^{-6} \qquad (7.1)$$

where T is the absolute temperature in Kelvin, p the air pressure in millibar et e the partial vapor pressure in millibar. For light waves, the terms in e are left out.

The observation of the atmosphere led to the definition of a "standard atmosphere", which is a statistical average (fig. 7.1).

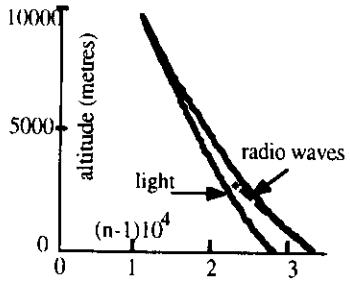

Fig. 7.1 Standard Atmosphere

The analysis of radio wave propagation in the atmosphere must determine how waves travel in heterogeneous media.

Propagation in stratif ed media

A continuous variation can be replaced, in first approximation, by a set of discrete but closely placed steps (fig. 7.2), and the standard expressions for transmission and reflection considered at each step. Accurate results may require many steps, and thus significant computation time and memory space requirements. In some particularly favorable cases, for instance when the variation occurs in one coordinate direction only, one can take the limit of vanishingly short steps and obtain an exact expression.

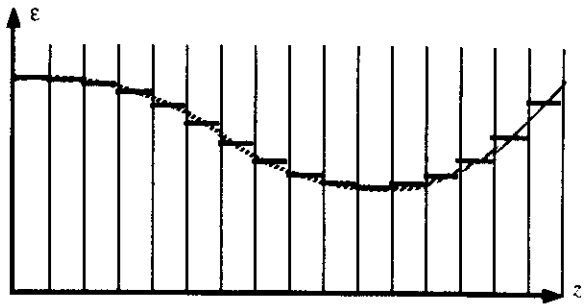

Fig. 7.2 Staircase Approximation

Determination of the path

For isotropic and lossless media, the angles of incidence θ_{in} and of transmission θ_t, both defined with respect to the normal to the interface, are related by Snell's law:

$$\sqrt{\varepsilon_1 \mu_1}\, \sin\theta_{in} = \sqrt{\varepsilon_2 \mu_2}\, \sin\theta_t \qquad (7.2)$$

where the indices 1 and 2 refer to the media on both sides of the 1-2 interface (fig.7.3).

Applying eqn. (7.2) to the successive interfaces, one gets :

$$n_0 \sin\theta_0 = n_1 \sin\theta_1 = n_2 \sin\theta_2 = n_3 \sin\theta_3 = \ldots \qquad (7.3)$$

where the media are assumed to be non magnetic, and the refractive index is defined as $n_i = \sqrt{\varepsilon_i / \varepsilon_0}$.

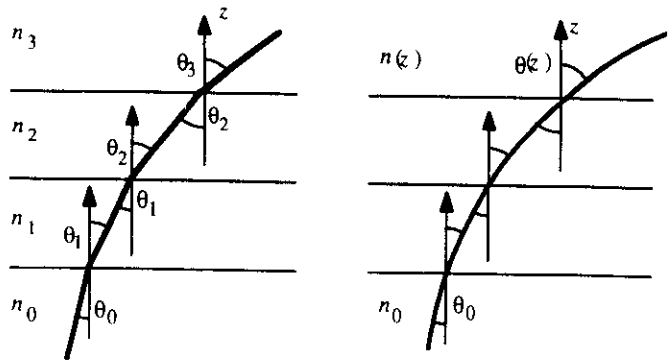

Fig. 7.3 Multiple interfaces and continuous variation

To find the propagation in a medium with continuous variation, the with of each layer is reduced down to zero. There are no longer any reflected waves, and only the path followed by the transmitted ray has to be considered. Taking the limit is here quite straightforward, and yields :

$$n(y)\sin\theta(y) = n_0 \sin\theta_0 \tag{7.4}$$

Total reflection (tangential horizontal path) is obtained for :

$$n(y_{max}) = n_0 \sin\theta_0 \tag{7.5}$$

Propagation over a spherical earth

The previous section considered flat interfaces, but radio wave propagates over a spherical earth, where the refractive index is a function of the radial coordinate r, the origin being located at the center of the earth. A somewhat similar situation is encountered in graded index optical fibers, where the index is a function of the radial circular coordinate ρ (however the sizes involved are different).

Over the interfaces between the successive media n_{i-1}, n_i et n_{i+1}, Snell's law is applied, yielding :

$$n_{i-1}\sin\theta_{i-1}^{+} = n_i \sin\theta_i^{-} \tag{7.6}$$

$$n_i \sin\theta_i^{+} = n_{i+1}\sin\theta_{i+1}^{-} \tag{7.7}$$

It was assumed that the curvature radii are very much larger than the wavelength, in which case Snell's law remains valid.

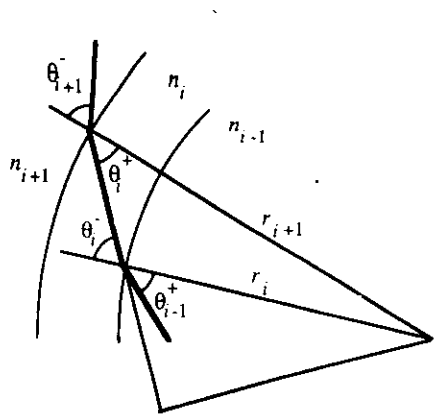

Fig. 7.4 Transmission across spherical (or cylindrical) shells

The two angles θ_i^- and θ_i^+ are not equal, so that these two equations do not have the same values (in contrast with eqn. 7.3)., If the trajectory (straight) in medium i is extended, and a perpendicular line drawn to the center, it is apparent that the projection of the two radii on the perpendicular yields :

$$r_i \sin\theta_i^{-} = r_{i+1}\sin\theta_i^{+} \tag{7.8}$$

Combining equations (7.6), (7.7) and (7.8) then yields for a continuous variation:

$$n(r) r \sin\theta(r) = n_0 r_0 \sin\theta_0 \tag{7.9}$$

The expression is rather similar to (eqn. 7.4), containing in addition the radial coordinate.

To study the propagation of radio or light waves in the atmosphere, the curved trajectories of the rays should be determined, which would be a rather complicated process. It is possible to simplify it considerably with some simple approximations.

Straight propagation over a fictitious spherical earth

Equation (7.9) is expressed in terms of the grazing angle $\alpha = 90^o - \theta$:

$$n(h)(a+h)\cos\alpha(h) = n_0\, a\cos\alpha_0 \qquad (7.10)$$

where a is the earth radius (6400 km), h the altitude above sea level, et α_0 the angle of the trajectory with an horizontal line at sea level. Since point-to-point radio propagation is generally very close to horizontal, some approximations can be made:

$$n\left(1+\frac{h}{a}\right)\left(1-\frac{\alpha^2}{2}\right) = n_0\left(1-\frac{\alpha_0^2}{2}\right) \qquad (7.11)$$

This expression is developed and only the first-order terms are retained:

$$\frac{1}{2}\left(\alpha^2-\alpha_0^2\right) \cong \frac{h}{a} + (n-n_0) \qquad (7.12)$$

The refractive index curve is then replaced by its tangent (fig. 7.1), yielding:

$$\frac{1}{2}\left(\alpha^2-\alpha_0^2\right) \cong \frac{h}{a} + (n-n_0) \cong \frac{h}{a} + h\,\partial_h n = \frac{h}{ka} \qquad (7.13)$$

Considering the last term on the right hand term in eqn. (7.13), one notices that it corresponds to propagation in an homogeneous medium (the term in $n - n_0$ has disappeared, but over a sphere of radius ka, where k is approximately equal to 4/3 for a standard atmosphere. The original problem, of curved rays over the real earth (which has the radius a) is replaced by straight rays over a "modified earth" having an equivalent radius ka (fig. 7.5). Straight lines are much easier to draw.

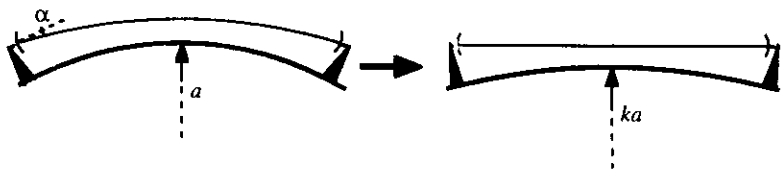

Fig. 7.5 From curved to straight propagation paths.

The topographic profile between the two antennas is then drawn on a chart corresponding to the modified earth. It is then possible to check whether the straight path is free from obstructions.

It should be noted that the "standard atmosphere" is not the same everywhere, so that the factor k may actually be different from 4/3 in some parts of the world.

Effect of ground reflection: Fresnel ellipsoid

Ground reflections contribute additional propagation paths between the two antennas, and reflected rays may thus interfere with the direct ray, either increasing or decreasing the amplitude of the received signal. To avoid such effects, it is recommended that there be no obstructions either within the Fresnel ellipsoid (fig. 7.6), which has the two antennas at its foci, and whose small half axis is given by:

$$b\,[\mathrm{m}] = 274\sqrt{\frac{d\,[\mathrm{km}]}{f\,[\mathrm{MHz}]}} \qquad (7.14)$$

where d is the distance between the two antennas (in kilometers) and where f is the signal frequency (in MHz).

Fig. 7.6 Fresnel ellipsoid

It is not always possible to select a path that is free from obstructions. In this case, the signal received is somewhat attenuated, by an amount that can be evaluated by considering how much of the ellipsoid cross-section is covered. The transmitted signal amplitude can then be increased to compensate for the attenuation resulting from scattering over obstacles.

Real atmosphere: anomalous propagation effects

One must still note that the standard atmosphere is a fiction, an approximate statistical representation of the actual profile, which may vary considerably with atmospheric conditions. In particular, inversion layers in the atmosphere may considerably modify wave propagation, acting as wave guiding channels (anomalous propagation). In the vicinity of such channels, silent zones appear, where signals mysteriously disappear, and may appear again as mirages at some further places. Anomalous propagation is encountered over hot desert areas and coastal zones, where different winds blow at different altitudes, coming from the coast or from the sea. Some (but of course not all) of the mysterious effects observed in the ill-famed "Bermuda triangle" are believed to result from anomalous propagation conditions.